UPPSALA
UNIVERSITET

Digital Comprehensive Summaries of Uppsala Dissertations from the Faculty of Science and Technology 910

Rate and Accuracy of Bacterial Protein Synthesis

MAGNUS JOHANSSON

ACTA
UNIVERSITATIS
UPSALIENSIS
UPPSALA
2012

ISSN 1651-6214
ISBN 978-91-554-8309-8
urn:nbn:se:uu:diva-171040

Dissertation presented at Uppsala University to be publicly examined in B41, BMC, Husargatan 3, Uppsala. Friday, May 4, 2012 at 09:30 for the degree of Doctor of Philosophy. The examination will be conducted in English.

Abstract
Johansson, M. 2012. Rate and Accuracy of Bacterial Protein Synthesis. Acta Universitatis Upsaliensis. *Digital Comprehensive Summaries of Uppsala Dissertations from the Faculty of Science and Technology* 910. 54 pp. Uppsala. ISBN 978-91-554-8309-8.

High levels of accuracy in transcription, aminoacylation of tRNA, and mRNA translation are essential for all life forms. However, high accuracy also necessarily means large energy dissipation and slow kinetics. Therefore, *in vivo* there is a fine tuned balance between rate and accuracy of key chemical reactions. We have shown that in our optimized *in vitro* bacterial protein synthesis system we have *in vivo* compatible rate and accuracy of ribosomal protein elongation. Our measurements of the temperature and the pH dependence of peptide bond formation with native substrates also suggest that the chemical step of peptidyl transfer, rather than tRNA accommodation, limits the rate of peptide bond formation. This work has made it possible to study ribosomal peptidyl transfer with *native* substrates.

Furthermore, we have developed a general theoretical model for the rate-accuracy trade-off in enzymatic reactions. When considering this trade-off for protein synthesis in the context of the living bacterial cell, where cognate aa-tRNAs compete for ribosome binding with an excess of non-cognate aa-tRNAs, the model predicts an accuracy optimum where the inhibitory effect of non-cognate substrate binding and the efficiency loss due to high discard rate of cognate aa-tRNAs are minimized. However, these results also show that commonly used biochemical systems for protein synthesis studies operate at exceptionally suboptimal conditions. This makes it difficult, if not impossible, to relate the biochemical data to protein synthesis in the living cell.

To validate our theoretical model we developed a method, based on variation of the concentration of Mg^{2+} ions in the buffer, to study the rate-accuracy trade-off of bacterial protein synthesis *in vitro*. We found a linear trade-off between rate and accuracy of tRNA selection on the ribosome, from which we could estimate the maximal accuracy. Exploiting this method for a complete set of single-mismatch readings by one tRNA species, we found simple patterns of genetic code reading, where the accuracy was highest for the second and lowest for the third codon position. The results bridge the gap between *in vivo* and *in vitro* protein synthesis and allow calibration of our test tube conditions to those of the living cell.

Keywords: protein synthesis, ribosome, peptidyl transfer, rate-accuracy trade-off, kinetics

Magnus Johansson, Uppsala University, Department of Cell and Molecular Biology, Structure and Molecular Biology, 596, SE-751 24 Uppsala, Sweden.

ISSN 1651-6214
ISBN 978-91-554-8309-8
urn:nbn:se:uu:diva-171040 (http://urn.kb.se/resolve?urn=urn:nbn:se:uu:diva-171040)

Kråkan: *Du är en ko Mamma Mu! En ko! Kor KAN inte cykla!*

Mamma Mu: *Mu, det är därför jag vill lära mig.*

List of Papers

This thesis is based on the following papers, which are referred to in the text by their Roman numerals.

I Johansson M., Bouakaz E., Lovmar M., Ehrenberg M. (2008) The kinetics of ribosomal peptidyl-transfer revisited. *Mol Cell*, **30**(5):589–598

II Johansson M., Ieong K.W., Trobro S., Strazewski P., Åqvist J., Pavlov M.Y., Ehrenberg M. (2011) pH sensitivity of the ribosomal peptidyl transfer reaction dependent on the identity of the A-site aminoacyl-tRNA. *Proc Natl Acad Sci U S A*, **108**(1):79–84

III Johansson M., Lovmar M., Ehrenberg M. (2008) Rate and accuracy of bacterial protein synthesis revisited. *Curr Opin Microbiol*, **11**(2):141–147

IV Johansson M., Zhang J., Ehrenberg M. (2012) Genetic code translation displays a linear trade-off between efficiency and accuracy of tRNA selection. *Proc Natl Acad Sci U S A*, **109**(1):131–136

Contents

Abbreviations

30S	The small subunit of a bacterial ribosome
50S	The large subunit of a bacterial ribosome
70S	The complete bacterial ribosome
SD	Shine-Dalgarno sequence
IF	Initiation factor
EF	Elongation factor
RF	Release factor
PTC	Peptidyl transferase center
aa	Amino acid
T_3	Ternary complex (aa-tRNA·EF-Tu·GTP)
PEP	Phosphoenolpyruvate

Introduction

The Central Dogma

All living cells are built, organized and controlled mainly by proteins. Proteins make up muscle fibers, hairs, and skin; work as receptors on cell walls transmitting external signals to the cell interior; transport molecules from one part of the cell or body to another; and, perhaps the most important feature, as enzymes catalyze and control almost all chemical reactions taking place inside the living cell. The enormous diversity among proteins is due to the 20 different amino acid (aa) building blocks arranged in a unique way in each different protein, with numbers ranging from approximately fifty to tens of thousands of amino acids. The sequence of amino acid residues in a protein is ultimately determined by the sequence of nucleotides in the DNA of the gene encoding it. As DNA is the genetic information passed on to progeny, the differences among and between species are to a large extent due to differences in protein sequences and levels. The information in the gene is copied, transcribed, into a messenger RNA (mRNA) molecule which subsequently is translated by the protein synthesis machinery, the ribosome, connecting the amino acids in the sequence according to the mRNA blueprint (Fig. 1), ultimately determined by the genetic code (Fig. 2). The different amino acids are brought to the polymerization site on the ribosome by their corresponding transfer RNA (tRNA) molecules, having a unique set of base triplet anticodons, for each amino acid, matching the base triplet codons on the mRNA. In this way, the mRNA code is read by the different tRNA molecules on the ribosome, one codon at a time, and the amino acids, linked to the different tRNAs, get attached to each other in a growing polypeptide. When the ribosome reaches the stop codon, the polypeptide is released and folds into the mature protein.

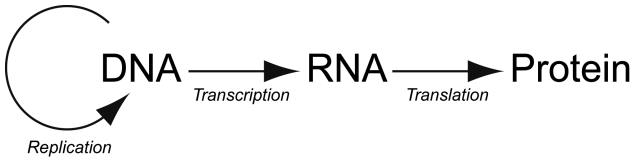

Figure 1. The central dogma of molecular biology. Protein encoding stretches of DNA (genes) are copied (transcribed) to RNA, serving as template for the synthesis of proteins on ribosomes (translation). The DNA content of a cell is replicated and passed on to progeny.

The mechanism described above, the central dogma of molecular biology, is in a way the quintessence of life as we know it. Although details differ, the overall design and mechanism of the transcription and translation machineries are very conserved throughout the whole tree of life, *i.e.* the ribosomes synthesizing proteins in *e.g. Mycobacterium tuberculosis* (the bacterium causing tuberculosis) work almost exactly in the same way as the ribosomes inside our own cells. In this thesis, mechanistic and functional aspects of protein synthesis in the bacterium *Escherichia coli* are considered. One could think of many reasons for using a bacterium, such as *E. coli*, for studies of protein synthesis. For example, many of all known antibiotics inhibit protein synthesis in the target bacteria, but one of the main reasons, I think, is because it's feasible. *E. coli*, normally thriving in our lower intestines, grows happily in the lab when well fed, and has been doing so for decades, why there is probably no other organism, including ourselves, that we have more detailed knowledge about. Genetic tools, such as transformation of, and protein expression from, recombinant DNA, have been available for a long time and are commonly used in any micro/molecular biology lab.

First position	Second position: U		Second position: C		Second position: A		Second position: G		Third position
U	UUU	Phe	UCU	Ser	UAU	Tyr	UGU	Cys	U
	UUC		UCC		UAC		UGC		C
	UUA	Leu	UCA		UAA	Stop*	UGA	Stop*	A
	UUG		UCG		UAG		UGG	Trp	G
C	CUU	Leu	CCU	Pro	CAU	His	CGU	Arg	U
	CUC		CCC		CAC		CGC		C
	CUA		CCA		CAA	Gln	CGA		A
	CUG		CCG		CAG		CGG		G
A	AUU	Ile	ACU	Thr	AAU	Asn	AGU	Ser	U
	AUC		ACC		AAC		AGC		C
	AUA		ACA		AAA	Lys	AGA	Arg	A
	AUG	Met**	ACG		AAG		AGG		G
G	GUU	Val	GCU	Ala	GAU	Asp	GGU	Gly	U
	GUC		GCC		GAC		GGC		C
	GUA		GCA		GAA	Glu	GGA		A
	GUG		GCG		GAG		GGG		G

* Stop codons read by release factors.
** AUG in start position of the mRNA encodes initiator tRNA.

Figure 2. The universal genetic code. On ribosomes, the nucleotide sequence of an mRNA molecule is translated into proteins according to the genetic code, where the sequence of nucleotide triplets determines the amino acid sequence in the protein.

Bacterial Protein Synthesis

During one generation time, typically around 20 min for *E. coli* grown in rich medium (Liang et al., 2000), the bacterial cell has to duplicate its complete set of proteins, making up approximately 55% of the cell dry mass (Neidhardt, 1987). To achieve this, the cell invests half of its dry mass into the protein synthesis machinery (Bremer and Dennis, 2008) and devotes the major fraction of its free energy dissipation (Russell and Cook, 1995) to the

synthesis of proteins. This means that there is a very large selection pressure on the rate of ribosomal peptide bond formation, since any mutation leading to higher growth rate will decrease the generation time and the mutant progeny will soon have outgrown all other cell lines. However, intuitively, high rate also means high error levels. Ribosomes tuned to high rate will necessarily make more errors in the form of incorrectly incorporated amino acids (Ehrenberg and Kurland, 1984; Kurland and Ehrenberg, 1984). Depending on where in the polypeptide chain the mistake is made, and also which amino acid substitution is made, the final protein will be more or less malfunctioning. To some extent the cell can of course cope with erroneous proteins, but at some level, the errors will start affecting the growth rate negatively. In other words, in living bacteria there is a trade-off between rate and accuracy of protein synthesis, and most certainly the protein synthesis machinery, including ribosomes, tRNAs and other translational factors, have evolved to optimize the growth rate by balancing the rate and the accuracy (Ehrenberg and Kurland, 1984; Kurland and Ehrenberg, 1984). In line with this hypothesis, mutant bacterial strains with hyper-accurate or error-prone ribosomes both grew more slowly than wild type cells (Tubulekas and Hughes, 1993). In *E. coli* growing in rich medium, the rate of protein synthesis is around 20 amino acids per second per ribosome (Liang et al., 2000), and this occurs at an error level equal to or less than one incorrectly incorporated amino acid per three thousand (Kramer and Farabaugh, 2007).

Overview of protein synthesis at the molecular level

The synthesis of a polypeptide on the ribosome according to the mRNA blueprint is conveniently divided into four stages (reviewed in (Schmeing and Ramakrishnan, 2009)): initiation, when the ribosome assembles around the start codon on an mRNA; elongation, when the ribosome reads the codons and polymerizes the polypeptide; termination at a stop codon when the polypeptide is cut off; and finally ribosome recycling when the ribosome disassembles and gets ready for a new round of protein synthesis.

Initiation

Protein synthesis is initiated by the association of the small ribosomal subunit (30S) to an mRNA (Fig. 3). To correctly position the mRNA, an anti-Shine-Dalgarno sequence of the 16S rRNA (the RNA constituent of the 30S ribosomal subunit) on the 30S subunit basepairs with the Shine-Dalgarno sequence (SD) of the mRNA. The protein initiation factor 3 (IF3) is likely to facilitate this mRNA binding step by keeping the 30S subunit from binding to the large ribosomal subunit (50S). Subsequently, the initiator aminoacyl-tRNA, fMet-tRNA^{fMet}, binds and basepairs with the help of initiation factors 1 (IF1) and 2 (IF2) to the AUG start codon of mRNA. The initiation phase is finally completed when the 50S subunit associates to

the complex and the initiation factors fall off, leaving the fMet-tRNA^{fMet} bound to the P (peptidyl) site of the now 70S ribosome, with the second codon to be read displayed in the available A (aminoacyl) site. The series of events is partly driven by the hydrolysis of IF2 bound GTP.

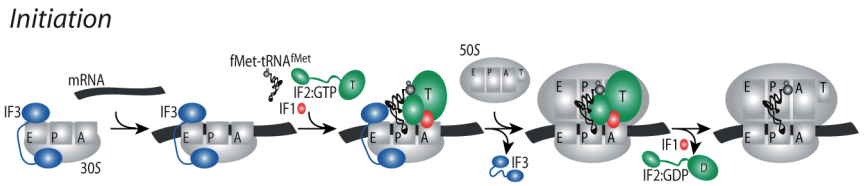

Figure 3. Initiation phase of translation.

Elongation

During the elongation phase, aminoacyl-tRNA in ternary complex (T_3) with elongation factor Tu (EF-Tu) and GTP binds to the A site of the 70S ribosome (Fig. 4). Upon correct codon-anticodon recognition, *i.e.* basepairing between the A-site codon and the tRNA anticodon, the EF-Tu bound GTP is hydrolyzed to GDP, inducing the dissociation of EF-Tu and the proper accommodation of the aa-tRNA into the A site. The ester bound amino acid is now pointing into the catalytic site of the 50S subunit, the peptidyl transferase center (PTC), where the synthesized polypeptide (or only fMet for the first round of elongation) is attached to the P-site tRNA. The peptide is then transferred from the P-site tRNA to the amino acid on the A-site tRNA by the formation of a peptide bond (the peptidyl transfer reaction, see further details below). EF-Tu is recycled by the rapid exchange of GDP to GTP, facilitated by elongation factor Ts (EF-Ts).

After peptidyl transfer, the ribosome has to take another step on the mRNA, so that the next codon to be read ends up in A site, and the tRNA, with the now one amino acid longer peptide attached, is moved to the P site. This event, the translocation step, is facilitated by elongation factor G (EF-G) and the hydrolysis of another GTP molecule. The exact mechanism of EF-G mediated translocation is still not clearly understood and there is some controversy on the subject. However, it is clear that the two ribosomal subunits have to rotate in relation to each other (Frank and Agrawal, 2000). This positions the tRNAs in “hybrid” state, E/P and P/A (as opposed to the “classical state” P/P and A/A, see figure 4). EF-G is then likely to bind and stabilize the rotated state of the ribosome and the tRNA-mRNA complex moves one step on the 30S subunit to again adopt a classical state, now E/E and P/P. The controversy lies in the role of the hydrolysis of EF-G bound GTP. It is clear that GTP hydrolysis must occur for the elongation to proceed, but it seems likely that the ribosome can translocate also with the non-hydrolysable GTP analogue GDPNP (Ermolenko and Noller, 2011). Hence, at this point it seems that GTP hydrolysis is only needed for the

dissociation of EF-G from the ribosome, and not to drive the intersubunit movement, as suggested previously (Rodnina et al., 1997). After translocation, the next codon to be read is displayed in the now again available A site and the elongation proceeds.

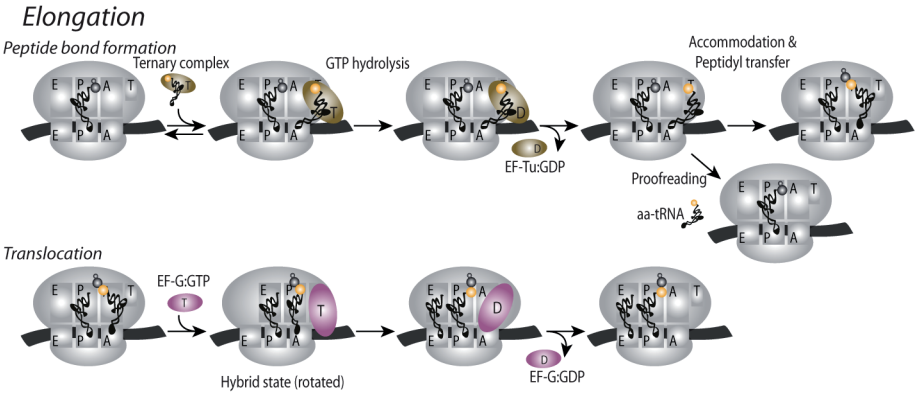

Figure 4. Elongation phase of translation.

Termination

When the A site displays a stop codon (UAG, UAA, UGA) there are no matching tRNAs that can bind. Instead a class I release factor (RF1 or RF2 depending on the stop codon) binds to the A site and stimulates the ribosome catalyzed hydrolysis of the ester bond between the last amino acid of the polypeptide and the P-site tRNA, releasing the polypeptide from the ribosome (Fig. 5). The GTP associated class II release factor 3 (RF3) then destabilizes the class I release factor and they both dissociate, leaving the 70S ribosome bound to mRNA and a now deacylated tRNA in P site.

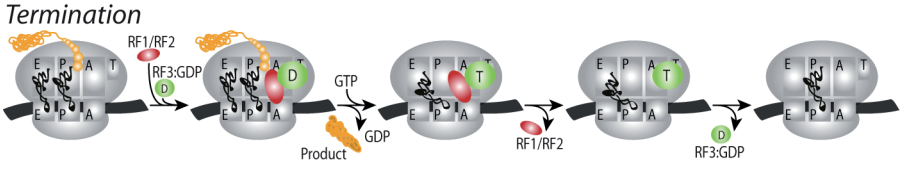

Figure 5. Termination phase of translation.

Ribosome recycling

In order to start a new round of protein synthesis the 70S ribosome is finally split by the ribosome recycling factor (RRF) and EF-G·GTP and subsequently held apart by the influence of IF3 (Fig. 6).

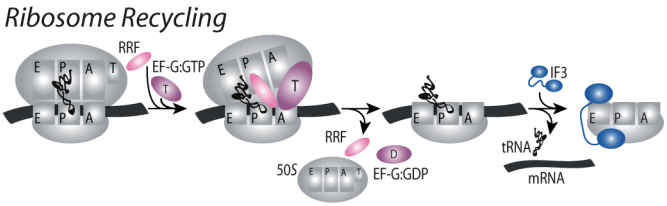

Figure 6. Ribosome recycling.

Accuracy of tRNA selection on the ribosome

The problem of substrate similarities

Already in the fifties it was pointed out that substrate similarities would lead to large error levels in biochemical pathways, such as protein synthesis or DNA replication (Pauling, 1957). Based on free energy differences of substrate binding, Pauling speculated that the small differences of *e.g.* the amino acids valine and isoleucine would not be sufficient to account for the extremely low error levels that had been measured for amino acid misincorporation into proteins. A possible solution to this apparent contradiction was presented independently by Hopfield and Ninio (Hopfield, 1974; Ninio, 1975). In brief their models proposed that the differences in substrate binding energies can be utilized twice by separating an initial selection of substrates from a subsequent proofreading step by coupling the reaction to some practically irreversible reaction. The model was later proven experimentally for amino acid charging on tRNAs by aminoacyl-tRNA synthetases (aaRS). Here it was shown that by utilizing the high energy bond in activated aminoacyl-adenylates, formed by the hydrolysis of ATP, an incorrect amino acid can be selected against by the aaRS, first as free amino acid, and then as the activated adenylate or after transfer to the tRNA (Fersht and Dingwall, 1979; Yamane and Hopfield, 1977). Since the concentration of ATP is kept far above equilibrium with AMP in the cell, the two (or three) selection steps are effectively separated making it possible for the aaRS to utilize the substrate differences multiple times.

Later, using reconstituted *in vitro* systems for protein synthesis, it was shown that a similar proofreading mechanism exists in the selection of tRNAs on the ribosome (Ruusala et al., 1982; Thompson and Stone, 1977). Here, hydrolysis of EF-Tu bound GTP marks the endpoint of the initial selection of aa-tRNA. Subsequently, EF-Tu·GDP falls off, and before peptidyl transfer occurs there is a possibility for the ribosome to discard the aa-tRNA a second time (Fig. 4). That is, by delivering the aa-tRNA to the ribosome in a complex with EF-Tu and GTP, and coupling the selection to hydrolysis of GTP, the correct codon-anticodon interaction can be tested for twice, first in the ternary complex, and then for the naked aa-tRNA.

Recent findings suggest also an additional mechanism, acting after peptide bond formation, which would help in maintaining low error levels in

bacterial protein synthesis (Zaher and Green, 2009, 2011). It was shown that once an error had been made, resulting in a mismatched peptidyl-tRNA in the ribosomal P site, the probability of making a second error increased. Interestingly, a codon-anticodon mismatch in the P site stimulated the hydrolytic effect of class I release factors on sense codons (aa encoding), and the effect was even more pronounced when there was a mismatch also in the E site and in the presence of RF3. That is, the results suggest that incorrect peptidyl transfer to a non-cognate aa-tRNA leads to accumulation of errors and eventually premature termination of translation. It should be noted, however, that error correcting mechanisms of this type are intrinsically wasteful and sometimes counter productive (Kurland and Ehrenberg, 1985).

Codon reading at atomic resolution

The molecular basis for the discrimination of codon-anticodon mismatches has been suggested from NMR structural data (Fourmy et al., 1996; Fourmy et al., 1998) and x-ray chrystallography (Ogle et al., 2001). Based on structures with or without error-inducing drugs (as will be discussed later), or with completely matched base triplet codon-anticodon interactions relative to structures where a single mismatch had been introduced, it was apparent that the ribosome "senses" the correct Watson-Crick basepairing in the first two codon positions with a so called A-minor interaction. That is, in a perfect RNA-RNA duplex, bases A1493 and A1492 of the 16S rRNA interact with the minor groove of the RNA-RNA helix (with the help of G530 of 16S rRNA). If the helix is somewhat disrupted, *e.g.* by the introduction of a mismatched pair in the first or second position, the minor groove gets slightly different and the A-minor interaction is disturbed. Further it was hypothesized that a proper codon-anticodon helix, involving the correct positioning of A1492, A1493, and G530, leads to a major conformational change of the 30S subunit (a domain closure of the 30S shoulder) and hence that the GTPase activity of the 50S subunit is triggered by signal transfer through the tRNA and EF-Tu (Cochella and Green, 2005; Ogle et al., 2001; Ogle and Ramakrishnan, 2005). This means that it is not only the stability of the triplet RNA duplex that is taken into account on the ribosome, but that this is amplified by a sensing of the correct geometry of the codon-anticodon interaction with proper Watson-Crick base pairing in the first two positions, leading to an accelerated GTPase activation for cognate substrate as had been seen in biochemical experiments (Pape et al., 1999). The model however also suggests that no such geometry sensing exists in the third codon position, explaining the partial degeneracy of this position in the genetic code (Fig. 2), in line with the wobble hypothesis, as formulated already by Crick (Crick, 1966).

Error inducing antibiotics

An important help in the process of unraveling the molecular details of tRNA selection on the ribosome comes from the usage of error inducing drugs. It has long been known that streptomycin, a member of the aminoglycoside family of antibiotics, induces errors in protein synthesis in living bacteria (Gorini et al., 1966). Bacterial strains carrying resistance to the drug usually have mutations in the ribosomal protein S12 (Ozaki et al., 1969). Interestingly, the resistant strains are to varying extent streptomycin dependent and hyper-accurate in translation in the absence of the drug (Bouadloun et al., 1983; Chakrabarti and Gorini, 1975). Thus, resistance was not caused by preventing the drug to bind, which is often the case in antibiotic resistance, but rather by compensating for the elevated antibiotic induced misreading by increasing the accuracy of the ribosomes. When selecting for compensatory mutations (Brownstein and Lewandowski, 1967), alterations in ribosomal protein S4 (or S5) were found (Zimmermann et al., 1971). The double mutant ribosomes were, both *in vivo* and *in vitro*, shown to behave like wild type, and by analyzing the single secondary mutants it was found that the compensatory effect was due to an introduction of an error-increasing mutation, causing similar effects like that of the drug (Bjare and Gorini, 1971; Brownstein and Lewandowski, 1967). The effect was later explained from structural data, where it was proposed that mutations in S12, part of the 30S shoulder domain discussed above, destabilize the closed form, and thus lead to less efficient GTPase activity and hence slower but more accurate ribosomes. On the other hand, the S4 mutants were shown to stabilize the closed conformation leading to decreased fidelity of tRNA selection. The wild-type behavior of the double mutants would then be considered as an evening out of effects. However, the model does not explain the nature of another set of double mutants (Bjorkman et al., 1999), where a combination of an S4 hyper-accurate mutant with an S12 hyper-accurate mutant also rendered wild-type behaving cells.

In vivo estimated error frequencies

In vivo error frequencies of protein synthesis have been studied thoroughly over the years, and an average missense error frequency of approximately $4 \cdot 10^{-4}$ has been suggested (Parker, 1989). More recently Kramer and Farabaugh developed a new sensitive approach to measure misreading frequencies (Kramer and Farabaugh, 2007). The method makes use of a firefly luciferase with an essential Lys residue in the active site. By mutating the gene at the Lys codon position, the misreading frequency of $tRNA^{Lys}$ on all possible single-mismatch codons could be estimated from the luciferase activity. One important finding of the study was that the error frequency varied drastically, with a few hotspots with high error frequency. However, due to relatively high background luciferase activity, possibly reflecting

errors in transcription, misacylation of tRNA, or more likely enzyme activity even in the absence of Lys, most single-mismatch error frequencies reported are probably over estimates.

In vitro estimated error frequencies

Also in reconstituted *in vitro* systems for protein synthesis, error frequencies have been estimated. In an *in vivo* like buffer system with energy regeneration components, optimized for rapid and accurate poly(Phe) synthesis on poly(U) in the presence of non-cognate Leu-tRNA^{Leu} isoacceptors (Jelenc and Kurland, 1979), Phe was incorporated into polypeptides at a rate of 10 s^{-1} (per ribosome) at a missense error frequency (Leu incorporation) of approximately 10^{-4} (Wagner et al., 1982). The system was later used to show that the misreading of UUU by Leu-tRNA$^{Leu2}_{GAG}$ also occurred at an accuracy of 10^4, with an equal contribution of 100 each from initial selection and proofreading (Ruusala et al., 1982). More recently a detailed scheme of the mechanism of ribosome catalyzed protein synthesis has been elucidated, now using heteropolymeric mRNAs. Taking advantage of stopped-flow and quench-flow techniques, with a combination of fluorescently labeled substrates and mutated elongation factors or non-hydrolyzable GTP analogues, M. Rodnina with coworkers have been able to dissect the elongation cycle into multiple discrete steps (Fig. 13) (Gromadski and Rodnina, 2004; Pape et al., 1998). From their assays, the individual steps where discrimination between correct and incorrect codon-anticodon interactions occur have been demonstrated, and among other things the accelerated GTPase activation upon correct codon-anticodon interaction, the "induced fit" hypothesis dicussed above, was found (Pape et al., 1999). However, the accuracy of tRNA selection in this system was one order of magnitude lower than that of the poly(U) system in earlier years.

Peptidyl transfer mechanism

Until recently very little was known about the mechanism of the chemistry of peptidyl transfer on the ribosome. This is very interesting since one could argue that the peptidyl transfer reaction is, together with the other polymerizing reactions of DNA replication and transcription, one of the truly fundamental reactions of life. One major reason for this difficulty of course lies in the bare size and complexity of the enzyme, the ribosome, and the involvement of complex biomolecule substrates, such as tRNA. However, in the beginning of this century several important high resolution x-ray crystal structures of the ribosomal subunits were solved (Ban et al., 2000; Schluenzen et al., 2000; Wimberly et al., 2000). From the positioning of the substrates it was now possible to make predictions about the mechanism (Hansen et al., 2002; Nissen et al., 2000; Schmeing et al., 2005) and also to make molecular dynamics simulations of the reaction (Trobro and Åqvist,

2005). It was first suggested that the catalytic activity of the ribosome is based on the proper positioning of the substrates, leading to reduced activation entropy (Hansen et al., 2002). This is in contrast to how most protein based enzymes work, where usually the activation enthalphy of the reaction is reduced by simplifying bond making and breaking by the introduction of chemical groups in the vicinity of the reactants taking part in the reaction. The entropy driven catalysis was later confirmed by Trobro and Åqvist (Trobro and Åqvist, 2005, 2006) using molecular dynamics simulations, but the cause of the energy barrier decrease rather seemed to stem from an ordered network of hydrogen bonds, involving two positioned water molecules, formed in the ground state and stable all the way up to the transition state, also suggested by (Schmeing et al., 2005).

The mechanism was at approximately the same time studied experimentally by investigation of the temperature dependence of ribosomal peptidyl transfer to the antibiotic puromycin, a small aa-tRNA mimicking molecule (Sievers et al., 2004). From the temperature dependence, and comparisons to a model for uncatalyzed peptidyl transfer, it was concluded that the catalysis indeed was due to a decrease in activation entropy. The reason why the experiments were carried out with puromycin rather than with full length aa-tRNA is that peptidyl transfer to native aa-tRNA is believed to be rate limited by the accommodation of aa-tRNA into the A site subsequent to GTP hydrolysis (Pape et al., 1998; Rodnina et al., 1994).

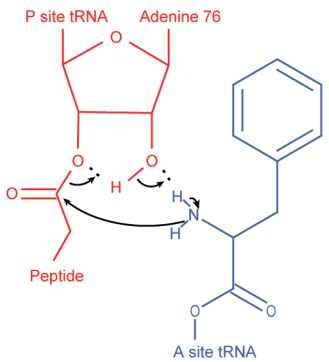

Figure 7. The proposed mechanism of peptidyl transfer on the ribosome (Schmeing et al., 2005; Trobro and Åqvist, 2005). A nucleophilic attack of the α-amino group of the A-site aa-tRNA (blue, here Phe-tRNA^{Phe}) on the ester carbonyl carbon of the P-site peptidyl-tRNA (red) results in a six-membered transition state.

Peptidyl transfer on the ribosome proceeds through a nucleophilic attack of the α-amino group of the amino acid attached to the A-site tRNA, on the ester carbonyl carbon of the P-site peptidyl-tRNA (Fig. 7) (Trobro and Åqvist, 2005). An obvious prediction from this model is that there should be a large effect of pH on the rate of the reaction. This is because the reactivity of the protonated ammonium form of the amino acid is likely to be

completely abolished. That is, by titrating the amino group to ammonium the reaction rate should get successively slower. Further, since the proposed mechanism does not involve general acid-base catalysis by ribosomal groups (Schmeing et al., 2005; Trobro and Åqvist, 2005), the pH dependence of the reaction rate should show the titration of only one reacting group. Experimental evidence for this hypothesis has been rather weak, as will be discussed further below.

The present work

Experimental Setup

In vitro system for protein synthesis

In our laboratory, a unique system for studying protein synthesis *in vitro* has been developed (Pavlov and Ehrenberg, 1996). Starting from *E. coli* cells, all known important players in translation are purified separately. Apart from ribosomes, the system includes: initiation factors 1, 2, and 3 (IF1, IF2, IF3): elongation factors Tu (EF-Tu), Ts (EF-Ts), and G (EF-G); all 20 aminoacyl-tRNA synthetases (each responsible for loading one amino acid out of 20 on its corresponding tRNA); release factors 1, 2, 3 (RF1, RF2, RF3); ribosome recycling factor (RRF); and a mixture of all tRNAs (some individually purified, and some purchased in semi-purified form). Synthetic mRNAs, resembling natural ones, are also produced in the laboratory using *in vitro* transcription of PCR amplified designed "genes" (Pavlov and Ehrenberg, 1996). By doing this, we can decide the sequence of amino acids to be assembled in our *in vitro* translation system. Most of the protein components are nowadays purified by affinity chromatoghraphy, *i.e.* they are expressed with a poly(His)-tag flanking the protein, making it stick to Ni-resin in a column. However, if one wants to run experiments under *in vivo* like conditions the more resemblance to nature the better. In all my experiments related to binding and processing of ternary complexes I have therefore used wild type EF-Tu.

The buffer system used was also developed in house (Jelenc and Kurland, 1979). It was designed and carefully optimized for *in vivo* like rates and accuracies of protein synthesis. Apart from a mixture of salts with *in vivo* like concentrations, the system includes positively charged polyamines known to bind and stabilize the negatively charged phosphate backbones of RNA and DNA. Since protein synthesis on the ribosome, as well as charging of amino acids on tRNAs, require energy in the form of hydrolysis of GTP and ATP, an energy regenerating system is also included. In my experiments there were always 2 mM in total of GTP and ATP (usually 1:1, but for practical reasons sometimes different ratios), 10 mM phosphoenolpyruvate (PEP), myokinase (MK, to convert AMP/GMP to ADP/GDP respectively by the use of ATP/GTP) and pyruvate kinase (PK, to rephosphorylate ADP and GDP to ATP and GTP, respectively, by the dephosphorylation of PEP). This

keeps ATP and GTP levels high and constant throughout the experiment, driving the reactions forward.

In order to detect the molecules, and thereby follow reactions, I have used radioactively labeled substrates. That is, by forming peptides using *e.g.* tritium ([^{3}H]) labeled amino acids, or using [^{3}H]GTP when making the ternary complex, one can follow the reactions by separating substrates from products (as will be discussed below) and measure the radioactivity.

Procedures

All experiments presented in this thesis are in principle performed in the same way. Reagents, *e.g.* initiated ribosomes and ternary complexes, are preformed separately by mixing and preincubating their respective constituents. The reaction is then started by mixing the two reagent mixtures and the time evolution of product formation is followed by quenching the reaction at different incubation times by the addition of *e.g.* formic acid. Acid precipitates RNA, so by centrifuging the samples it is possible to separate radiolabeled amino acids and peptides bound to tRNAs, *e.g.* f[^{3}H]Met and f[^{3}H]Met-Phe, in the pellet from radiolabelled nucleotides, *e.g.* [^{3}H]GTP and [^{3}H]GDP, in the supernatant. The amino acids and peptides are then cut off from the tRNAs by potassium hydroxide mediated hydrolysis of the ester bond and finally separated from the RNAs and proteins by subsequent precipitation and centrifugation. To quantify the level of products, *i.e.* [^{3}H]GDP and f[^{3}H]Met-Phe in the example, the compounds are separated using HPLC. [^{3}H]GTP and [^{3}H]GDP are separated on a MonoQ ion-exchange column and f[^{3}H]Met is separated from f[^{3}H]Met-containing dipeptide on a C18 RP-HPLC column. By having a scintillation counter connected to the output from the HPLC, the levels of radioactively labeled compounds are detected and recorded online.

In paper I [^{3}H]GTP and [^{3}H]GDP were separated by Thin Layer Chromatography (TLC). This method was less sensitive, *i.e.* the radioactivity signal was weaker, and it was also less reproducible. For paper II (and simultaneous work by M. Pavlov (Pavlov et al., 2009)) we therefore developed the method of HPLC separation of nucleotides.

Except for measurements of misreading events, the reactions I've been trying to follow are all very fast. A typical dipeptide reaction between ternary complex and ribosomes programmed with the cognate codon in A site takes 10-100 ms. Of course this is impossible to follow stepwise by quenching the reaction by hand, *i.e.* adding acid at different time points. Instead we use a quench-flow instrument when doing these experiments. A quench-flow instrument is a computer controlled motor rapidly pushing reagents in thin tubing allowing them to react only for a preset time, after which they are mixed with a quenching liquid (Fig. 8).

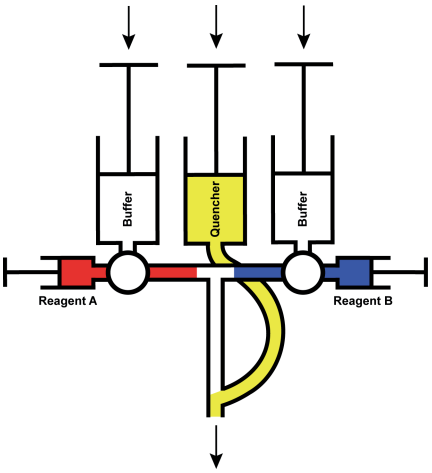

Figure 8. In a quench-flow instrument, reagents (blue and red) are rapidly mixed and allowed to react for a preset time. The reaction is then quenched by the addition of a quencher liquid, *e.g.* formic acid (yellow), and the sample expelled into a tube.

Rate of ribosomal peptidyl transfer

Rate limiting step

Due to the strong selection pressure on the elongation rate of mRNA translation on the ribosome, the parameters that govern the rate of the slowest steps in the cycle must have been optimally tuned by evolution. We do know that the *average* rate of elongation in living *E. coli* is 22 aa/s (Liang et al., 2000), but whether the actual rates vary considerably depending on codons/amino acids is not known. Neither is it known what step is actually rate limiting. Limiting levels of aminoacyl-tRNAs would make the binding rate of ternary complex small. Other possibilities include hydrolysis of EF-Tu or EF-G bound GTP, the chemical step of peptidyl transfer, or the movement of mRNA/tRNAs during translocation. The rate limiting step might also change depending on growth conditions, *e.g.* during starvation of a specific amino acid the level of the corresponding aa-tRNA would be low resulting in low concentration of the ternary complex and hence slow association. From *in vitro* experiments in the laboratory of M. Rodnina the prevailing conclusion was that the rate limiting step in ribosomal peptide bond synthesis is aa-tRNA accommodation into the A site subsequent to hydrolysis of EF-Tu bound GTP. The rate of accommodation was reported to be 2-10 s^{-1} at 20°C as well as at 37°C (Beringer et al., 2005; Bieling et al., 2006; Gromadski and Rodnina, 2004; Hesslein et al., 2004). An immediate conclusion one can draw from these results is that the experimental setup does not reproduce *in vivo* conditions very well, since in a sequence of steps with an overall rate of 22 s^{-1}, there cannot be any single step slower than

22 s^{-1}. Another problem with their experimental setup (later adopted by others (Cochella and Green, 2005; Zaher and Green, 2010)), is the apparently low accuracy of the system. The error frequencies reported, *e.g.* 1/450 (Gromadski and Rodnina, 2004), are too high to represent anything *in vivo* like where the average mistranslation frequency is estimated to 1/3300 or probably less (Kramer and Farabaugh, 2007; Parker, 1989). That is, despite the development of a more *in vivo* like system, with heteropolymeric mRNAs, the system developed in the laboratory of M. Rodnina and W. Wintermeyer did not seem to reproduce nature as well as the older model systems (Jelenc and Kurland, 1979; Wagner et al., 1982).

tRNA accommodation

The notion of a slow aa-tRNA accommodation step, preceeding the chemical step of peptidyl transfer, originates from experiments with fluorescently labeled tRNA molecules. Yeast $tRNA^{Phe}$ (*S. cerevisiae*), labeled with the fluorescent dye proflavine in position 16 or 17, in ternary complex with EF-Tu (*E. coli*) and GTP were reacted with poly(U) programmed *E. coli* ribosomes (Pape et al., 1998; Rodnina et al., 1994). The fluorescence signal, measured in a stopped-flow instrument, displayed two major fluorescence changes, where the first signal increase, attributed to GTPase activation, was followed by a slower signal decrease attributed to tRNA accommodation. The biphasic signal did not depend on whether the P-site tRNA was acylated or deacylated (data not shown by the authors); hence the signal reported events prior to (or non-related to) peptidyl transfer. Addition of the antibiotic kirromycin, known to inhibit dissociation of EF-Tu·GDP from the ribosome (Parmeggiani and Swart, 1985), trapped the compound in a high fluorescent state (Rodnina et al., 1994). Finally, the rate of peptide bond formation of 7 or 8 s^{-1} (depending on the Mg^{2+} concentration), as measured in quench-flow using *E. coli* $tRNA^{Phe}$, was approximately the same as that of the slow fluorescence decrease for the yeast $tRNA^{Phe}$(Prf16/17), 8 and 10 s^{-1} respectively (Pape et al., 1998). From my point of view, there are at least three possible problems with this analysis. First of all, as mentioned previously, one single step cannot be slower than the overall sequence of steps. Earlier it had been shown that the poly(U) based translation system indeed showed *in vivo* compatible rates (Bilgin et al., 1992; Wagner et al., 1982), indicating a possible problem with the new system. Secondly, the starting material for the labeled tRNA was from yeast, whereas ribosomes, translational factors and the $tRNA^{Phe}$ for quench-flow analysis were all of *E. coli* origin. Thirdly, the concentration dependence of *both* fluorescence phases, *i.e.* rapid increase and slow decrease (Fig. 4 in (Rodnina et al., 1994), Fig. 2C in (Pape et al., 1998)), is to my knowledge *not* compatible with a scheme where the two fluorescence signaling states are separated by an, in principle, irreversible GTP hydrolysis step (Fig. 13). That is, there is

either some serious problem in the parameter fitting procedure, or the tRNA attached proflavin dye reports on some step irrelevant to peptide bond formation. In paper I we aimed at, first of all, showing that peptide bond formation can indeed be very fast in the test tube, even in a heteropolymeric mRNA based system, and second, by analyzing the activation energies of the process, we were hoping to be able to say something about which step in the sequence of reactions is in fact the slowest.

Temperature dependence of peptidyl transfer (Paper I)

According to transition state theory, the rate, k, of a chemical reaction depends on the absolute temperature, T, according to:

$$k = \kappa \cdot \frac{k_B \cdot T}{h} e^{-\frac{\Delta H^{\ddagger}}{R \cdot T} + \frac{\Delta S^{\ddagger}}{R}} \quad (1)$$

Here, R is the gas constant, k_B Boltzmann's constant, h Planck's constant and κ the transmission factor, *i.e.* the probability of going to product rather than back to substrate at the transition state. $\Delta H^{\ddagger}$ is the activation enthalpy of the reaction and $\Delta S^{\ddagger}$ is the activation entropy. Setting $\kappa = 1$ in accordance with (Sievers et al., 2004) and rearranging, brings expression (1) into the form:

$$R \cdot ln\left(\frac{k \cdot h}{k_B \cdot T}\right) = \Delta S^{\ddagger} - \frac{\Delta H^{\ddagger}}{T} \quad (2)$$

This equation had been used before (Sievers et al., 2004) to estimate the activation enthalpy and entropy from the temperature dependence of the puromycin reaction (Table 1). From comparison with an uncatalyzed model reaction (Table 1) the conclusion was drawn that the catalytic activity of the enzyme is due to lowering of the activation entropy rather than the activation enthalpy. Our idea was then: if the chemical step of peptidyl transfer from native fMet-tRNA^{fMet} in P site to *native* aa-tRNA in A site is not masked by the preceding step of aa-tRNA accommodation, then by doing such a temperature dependence analysis with our native substrates we would probably get similar numbers as for the puromycin reaction, which is not rate limited by accommodation.

Experimental results

Thus, ternary complex, T_3, consisting of Phe-tRNA^{Phe}, GTP and EF-Tu, in excess was reacted with initiated 70S ribosomes, carrying f[^{3}H]Met-tRNA^{fMet} in P site and displaying the Phe codon UUU in A site. The time evolution of the reaction was followed using quench-flow, and the overall dipeptide formation rate was estimated at different concentrations of T_3 (Fig. 9A). By fitting these dipeptide formation rates, k_{dip}, to the Michaelis-Menten equation:

$$k_{dip} = \frac{[T_3] \cdot k_{cat}}{K_m + [T_3]}, \quad (3)$$

the rate of the reaction at saturated binding, k_{cat}, and the substrate concentration at which half maximal rate is achieved, K_m, were estimated (Fig. 9B). This was repeated at five different temperatures, 10°C to 37°C, and the estimated k_{cat} values ranged from 8.5 s^{-1} at low temperature up to 130 s^{-1} at physiological temperature of 37°C.

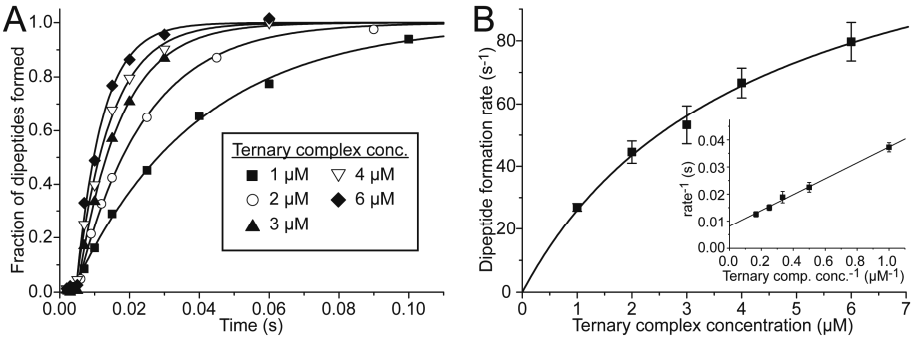

Figure 9. Dipeptide formation rates at 37°C. *Panel A*. Time courses of dipeptide formation at different substrate concentrations. *Panel B*. Rate of dipeptide formation at different substrate concentrations. The curve represents fitting of the data to the Michaelis-Menten equation (Eq. 3). *Insert*. Lineweaver-Burke plot of the same data.

This result by itself was already important, since the rate of dipeptide formation from other laboratories had been reported to be around 10 s^{-1} (Beringer et al., 2005; Bieling et al., 2006; Gromadski and Rodnina, 2004; Hesslein et al., 2004) as already discussed. By request from reviewers when the manuscript was submitted, we also had to repeat the experiments using the system of the laboratory of M. Rodnina. Interestingly, by using their weak SD mRNA, their high Mg^{2+} concentration buffer, and their way of titrating with ribosomes in excess over T_3 rather than the opposite, we could *not* reproduce their low k_{cat} values. However, we did notice that one possible explanation for the discrepancies could be that at the assumingly saturated substrate concentration used, 1 µM at 20°C and 0.6 µM at 37°C (Beringer et al., 2005; Bieling et al., 2006; Gromadski and Rodnina, 2004; Hesslein et al., 2004) the binding is far from saturated in our hands (Fig. 5 in paper I). In 2010 our fast kinetics were also reproduced in the laboratory of M. Rodnina (Wohlgemuth et al., 2010).

Even if the overall rate of peptide bond formation is limited by the chemistry of peptidyl transfer, there could be a significant influence of other steps. In order to minimize these kinds of errors, but still without introducing artificial dye labels, non-hydrolyzable nucleotide analogues, EF-Tu mutants or similar possible artefacts, we also measured the rate of the other step including breaking or formation of a covalent bond in the sequence, namely

hydrolysis of the EF-Tu bound GTP. By running the reactions with ^{3}H labeled GTP, and at near-saturating conditions, the time contribution from the steps up to and including GTP hydrolysis, $\tau_{cat}^{(GTP)}$, to the overall time of dipeptide formation, $\tau_{cat}^{(dip)}$, could be subtracted, yielding the time for all steps subsequent to GTP hydrolysis, τ_{pep}:

$$\tau_{cat}^{(dip)} - \tau_{cat}^{(GTP)} = \tau_{pep} = \frac{1}{k_{pep}} \tag{4}$$

The inverse of τ_{pep}, k_{pep}, then is the compounded rate of the hypothetical tRNA accommodation step and the chemical step of peptidyl transfer.

Next, we plugged in our k_{pep} values measured at different temperatures into equation 2, and from the apparent straight line achieved when plotting the left hand side of the equation versus the inverted temperature (Fig. 10, black squares) we estimated the activation enthalpy and entropy as 17.0 and 2 kcal/mol respectively. As can be seen from Table 1 these numbers are strikingly similar to the ones measured for the puromycin reaction (Sievers et al., 2004). Unless aa-tRNA accommodation, for which no such quantitative data are available, has very similar activation energies as the puromycin reaction, this indicates that the rate limiting step in the sequence from T_3 binding to the ribosome up to and including peptidyl transfer is the chemical step of peptidyl transfer itself.

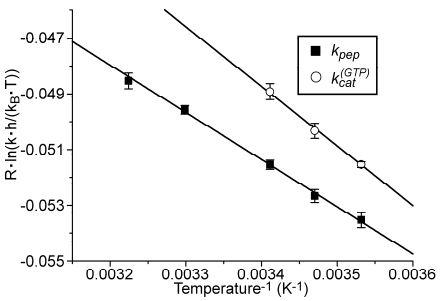

Figure 10. Temperature dependence of the compounded rate constant k_{pep} (accommodation and peptidyl transfer) and the saturated GTP hydrolysis rate, $k_{cat}^{(GTP)}$, plotted according to equation 2. From the straight line fits, estimates of $\Delta S^{\ddagger}$ and $\Delta H^{\ddagger}$ were obtained.

Finally, in paper I we also showed for one case, $tRNA^{Phe}$ reading its cognate UUU codon rather than its non-cognate CUU codon, that the accuracy of mRNA translation in our polymix based system, now using heteropolymeric mRNAs, was compatible with *in vivo* reported accuracies.

Table 1. Activation energies for peptidyl transfer

	Peptidyl transfer (k_{pep})	Puromycin reaction *	Uncatalyzed peptidyl transfer **
$\Delta G^{\ddagger}$ (kcal/mol)	15.08 ± 0.04	16.5	23.5 ± 0.7
$\Delta H^{\ddagger}$ (kcal/mol)	17.0 ± 0.9	17.2 ± 0.9	7.8 ± 0.4
$T\Delta S^{\ddagger}$ (kcal/mol)	2 ± 1	0.7 ± 0.2	-15.7 ± 0.8

* Data from (Sievers et al., 2004).

** Data from (Schroeder and Wolfenden, 2007).

pH dependence of peptidyl transfer (Paper II)

Paper II was a follow up on the results in paper I. Since it is not completely sure that puromycin behaves as a perfect mimic of aa-tRNA in the peptidyl transfer reaction (see further discussion below) or that the similarities between activation energy parameters (Table 1) were not just a coincidence, we needed to test the hypothesis from paper I in a different way. As pointed out earlier, a hypothesis from the proposed model for peptidyl transfer on the ribosome (Schmeing et al., 2005; Trobro and Åqvist, 2005) was that since the mechanism does not involve general acid-base catalysis, and since no ribosomal residues were supposedly involved in the proton shuttle mechanism, the pH dependence of the reaction should show *one* proton in an essential reacting group being titrated, *i.e.* the α-amino group of the A-site aminoacyl-tRNA. Since the mechanism of peptidyl transfer involves a nucleophilic attack of the α-amino group on the ester carbonyl carbon of the P-site peptidyl-tRNA, protonation of the α-amino group to an ammonium would almost completely abolish the reaction (Fig. 7). That is, by titrating free protons in the buffer, peptidyl transfer would get slower at lower pH, and faster as the pH is increased, until it reaches the maximal rate at complete deprotonation of the α-amino group. These experiments had been tried in the laboratory of M. Rodnina but also in the laboratory of R. Green. In line with the notion of slow aa-tRNA accommodation the rate of dipeptide formation with native Phe-tRNA^{Phe} did not show any significant pH dependence, 2-7 s^{-1} (scattered) in the pH range of 6-8 (Bieling et al., 2006). The rates were also indistinguishable from the rate of aa-tRNA accommodation, as measured in stopped-flow with Phe-tRNA^{Phe}(Prf16/17) or fluorescence resonance energy transfer (FRET, between fluorescein labeled fMet-tRNA^{fMet} and quencher labeled Phe-tRNA^{Phe}) which also did not show any significant pH effect. Instead the pH dependence on the peptidyl transfer mechanism was studied using puromycin and puromycin analogues. For these substrates, the pH-dependence is complex, with the

effect of *two* protons on the rate of peptidyl transfer to puromycin at 37°C (Beringer and Rodnina, 2007; Katunin et al., 2002) as well as at 20°C (Brunelle et al., 2006). The effect of two protons or one proton was observed for C-puromycin (natural puromycin attached to cytidine, resembling the terminal CCA of aminoacyl-tRNA better) at 37°C (Beringer and Rodnina, 2007) or 20°C (Brunelle et al., 2006), respectively. Furthermore, the rate of peptidyl transfer to CC-puromycin displayed a qualitatively different and much weaker pH-dependence (Beringer and Rodnina, 2007). In other words, from the experiments at hand no clear conclusions concerning peptidyl transfer could in fact be drawn, and they also suggest that care should be taken when interpreting data obtained from the puromycin reaction. The latter also becomes clear from studies of peptidyl transfer on ribosomes mutated in the rRNA of the PTC (Youngman et al., 2004). Here the rate of peptidyl transfer to puromycin, 10 s^{-1}, was reduced 30- to 9000-fold for the ribosome mutants, whereas the rate of peptide bond formation to Phe-$tRNA^{Phe}$, 2 s^{-1}, was unaffected or reduced only two-fold, meaning that puromycin is way far from being a perfect aa-tRNA analogue.

Since we had already shown that in our system (or in our hands?) peptide bond formation to native aa-tRNA was much faster than the reported rates from other groups, and also that to saturate the reaction a relatively high substrate concentration was needed, we suspected that the absence of pH dependence reported in (Bieling et al., 2006), and also the small nominal rates, could be due to subsaturating conditions. This would mean that the pH independence observed only tells us that the binding rate of T_3 to the ribosome is not affected by a change in pH. Hence we set off to measure the pH dependence of peptidyl transfer to native Phe-$tRNA^{Phe}$.

Experimental results

Also in these experiments we were only interested in the steps subsequent to GTP hydrolysis. However, instead of repeating the cumbersome titrations, as in paper I, to estimate k_{cat} values, we realized that we could in fact follow both GTP hydrolysis and peptidyl transfer in the *very same reaction*. Then, by subtracting the time for GTP hydolysis, τ_{GTP}, including the binding step, from the overall time, τ_{dip}, we would get a very precise estimate of the time, τ_{pep}, for all steps subsequent to GTP hydrolysis, from one single experiment (Fig. 1 in paper II). This method made the experiments much quicker and, more importantly, also the precision in parameter estimation improved drastically. From such experiments we estimated k_{pep} for peptidyl transfer (and accommodation) at different pH (Fig. 11). The curve in figure 11 represents the data fitted to a model where the rate of the reaction, k_{pep}, depends on the extent of protonation of a single reaction essential group:

$$k_{pep} = \frac{k_{pep}^{max}}{1 + 10^{\left(pK_a^{obs} - pH\right)}} \quad (5)$$

Here, k_{pep}^{max} represents the rate of the reaction at completely deprotonated form of a reacting group, and pK_a^{obs} is the pH at which half the maximal reaction rate is achieved. From this result we concluded that indeed we do see pH dependence of the steps subsequent to GTP hydrolysis, seemingly contradicting previously published results (Bieling et al., 2006). However as the rate changed only approximately twofold in the pH range measured, the effect would have been completely masked at the 2-7 s^{-1} precision reported earlier (Bieling et al., 2006).

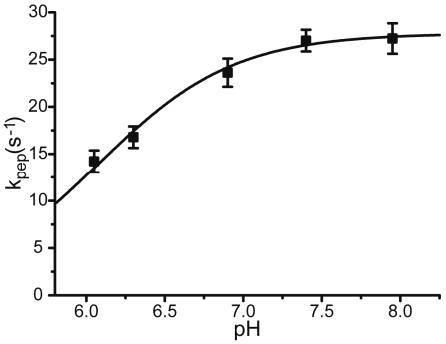

Figure 11. The compounded rate constant k_{pep} (tRNA accommodation and peptidyl transfer) measured at different pH for fMet-Phe dipeptide formation at 20°C. The curve represents the data fitted to a model where one reaction essential group is titrated with pH (Eq. 5).

One obvious problem with the results in figure 11 is that at neutral pH, the reaction rate is already close to its maximum. To overcome this problem, a substrate with higher pK_a of the reaction essential group was needed. Of the 20 canonical amino acids, the pK_a of the α-amino group is highest for proline (Pro) and lowest for asparagine (Asn) (Fersht, 1999). Hence, if the proton titration curve (Fig. 11) represents proton titration of the α-amino group of the A-site Phe-$tRNA^{Phe}$, this would in the pH range measured show a stronger pH dependence for Pro-$tRNA^{Pro}$ (higher pK_a) and weaker pH dependence for Asn-$tRNA^{Asn}$ in the A site. We also included Ala-$tRNA^{Ala}$, Ile-$tRNA^{Ile}$ and Gly-$tRNA^{Gly}$, with pK_as between those of Pro-$tRNA^{Pro}$ and Asn-$tRNA^{Asn}$ in the study. As can be seen in figures 3B-3G in paper II and in Table 2 (column 3) the results from the pH variation experiments were compatible with our hypothesis – the lowest pK_a was observed for peptidyl transfer to Asn and the highest pK_a for peptidyl transfer to Pro. Additionally, as can be seen in figure 3H in paper II, where the same data is plotted in log-scale, the k_{pep} variation for Pro and Gly with pH show a slope of one, meaning that one proton is being titrated, giving further support to the

proposed non-acid-base-catalyzed reaction mechanism (Schmeing et al., 2005; Trobro and Åqvist, 2005).

Table 2. pH dependence of k_{pep} for different aminoacyl-tRNAs at 20°C

Aminoacyl-tRNA	pK_a^{aq} *	pK_a^{obs}	k_{pep}^{max} (s^{-1})	k_{pep}^{phys} (s^{-1}) **
Asn-tRNA^{Asn}	6.8	5.9 ± 0.2	11 ± 1	11 ± 1
Phe-tRNA^{Phe}	7.2	6.1 ± 0.1	28 ± 1	27 ± 1
Ile-tRNA^{Ile}	7.8	6.1 ± 0.2	22 ± 1	21 ± 1
Ala-tRNA^{Ala}	7.9	6.3 ± 0.1	25 ± 2	24 ± 1
Gly-tRNA^{Gly}	7.8	7.36 ± 0.04	13 ± 1	7.6 ± 0.2
Pro-tRNA^{Pro}	8.6	7.8 ± 0.2	17 ± 5	6.0 ± 0.5

* pK_a of the α-NH_2 group of aa-tRNA in bulk water (see paper II).

** k_{pep}, calculated at pH 7.5 from fits of experimental data (Figs. 3B-G in paper II).

There was however yet another problem with these results. The observed pK_as were all lower than for the corresponding free amino acids. Even when the free amino acid pK_as were adjusted according to temperature and to represent ester bound amino acids (column 2 in Table 2) we still had apparent pK_a downshifts varying between 0.4 and 1.7 pH units. This could be due to authentic differences between α-amino group pK_as for small and large aminoacyl-esters or differences in pK_a on and off the ribosome, but it could also be due to the influence of a pH independent step prior to peptidyl transfer, *e.g.* tRNA accommodation. Since our kinetic analysis could not distinguish between these two possibilities (see detailed analysis in Supporting Information for paper II), this was a major concern. Significant help on this matter came from molecular dynamics simulations made in the laboratory of J. Åqvist. Stefan Trobro and Johan Åqvist were able to calculate hypothetical differences in α-amino group pK_as based on free energy differences from simulations of the protonated and deprotonated aminoacyl-tRNA variants on and off the ribosome. From detailed balance in such a thermodynamic cycle (Scheme S1 in paper II), the change in free energy differences of the protonated and deprotonated form, and hence the difference in pK_as, on and off the ribosome could be estimated. Due to limitations of the simulation system, absolute numbers of free energy differencies are impossible to get. Thus, the calculated pK_a shifts were fitted to the experimentally observed pK_a shifts, using the unknown dielectric scaling constant of the PTC surroundings as a fitting parameter. As can be seen in figure 12 there is a strong correlation between calculated and experimentally observed pK_a downshifts. In addition, snapshots from the

molecular dynamics simulations also give possible explanations for the pK_a downshifts for the tested amino acids. When the aminoacyl-tRNA is put in the PTC, the pK_a of the α-amino group decreases due to destabilization of the ammonium form relative to the amino form because of occlusion of water molecules. However, due to the absence of a side chain on Gly, a water molecule can enter the volume, providing solvation and thus explaning the lower downshift for this amino acid (see figure 5 in paper II).

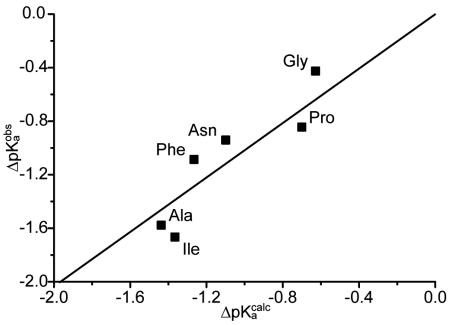

Figure 12. Experimentally observed shifts in pK_a of the α-amino group of aa-tRNAs on the ribosome relative to aa-tRNAs in bulk water, ΔpK_a^{obs}, plotted versus MD-simulated shifts, ΔpK_a^{calc}, in the pK_a value of aa-tRNAs as they move from bulk water to the ribosomal A site.

All together, the pH dependence of k_{pep}, which varies with the identity of the A-site aminoacyl-tRNA according to predictions from pK_as of free amino acids, and the correlation of observed and calculated pK_a downshifts, strongly support our hypothesis in paper I, namely that peptide bond formation on the ribosome is rate limited by the chemistry of peptidyl transfer itself. The results show that it is indeed possible to study peptidyl transfer from native peptidyl-tRNA to native aa-tRNA at physiological pH (7.5). This is clearly evident for $tRNA^{Gly}$ and $tRNA^{Pro}$, where the big variation of k_{pep} around pH 7.5 shows rate limiting chemistry, but could also very well be true for the other aa-tRNAs as suggested from the fits of the data to the single-proton-titration model (Fig. 3 in paper II), and from the correlation between observed and simulated pK_a downshifts (Fig. 12).

Further discussion of tRNA accommodation

Apart from the original studies (Pape et al., 1998; Rodnina et al., 1994) very little evidence for slow aa-tRNA accommodation has been presented. In a report from the laboratory of B. Cooperman, in a supplemental figure with lack of experimental details, it was shown that by having the proflavin label on the P-site tRNA the time evolution of the fluorescence signal was essentially the same as with the label on the incoming aa-tRNA. However, the rate of whatever triggered the fluorescence change was in both

experiments extremely small, 3 s^{-1} (Pan et al., 2007). One possible explanation for these small rates is that in such a fluorescence time course, the sequence of signals, analyzed as a number of exponential terms, does not necessarily reflect the actual sequence of events. That is, at sub-saturating conditions, the slowest step will be the binding reaction, and this will inevitably show up as the *longest lasting* exponential phase. However, in the literature the "slow fluorescence decrease" signal of proflavin is interpreted as to reflect the rate of tRNA accommodation (Bieling et al., 2006; Pape et al., 1998; Rodnina et al., 1994). This argument gets particularly interesting in a recent report from the laboratory of M. Rodnina (Wohlgemuth et al., 2010). Here, when trying to justify their previous accommodation arguments the authors show a fluorescence time curve where the slow phase, explained by the authors to represent tRNA accommodation, occurs at a rate of 40 s^{-1}, exactly the same rate as the dipeptide formation rate in a quench-flow experiment performed in parallel using the same reaction mixtures. This, they claim, shows that accommodation is fast but still limits peptidyl transfer. However, in the very same paper the authors present (when showing that they can reproduce our fast kinetics reported in paper I) a rate of peptide bond formation at saturating conditions, k_{cat} (called k_{dip} by the authors), of 174 s^{-1}. This means that in the very same buffer conditions as in the fluorescence experiment, the tRNA accommodation rate is at least 174 s^{-1}. That is, the proflavin experiment, most probably reflecting a slow binding reaction at subsaturating conditions, does not prove tRNA accommodation limited peptidyl transfer at all.

The problem has also been tackled from a completely different point of view. The idea of slow accommodation has led people to search for an "accommodation corridor" through which the aa-tRNA has to be threaded in order to accommodate properly, hence the slow rate. However, when mutating hypothetical key residues in this "corridor", picked up to be important from molecular dynamics simulations (Sanbonmatsu et al., 2005), no effect of the rate of peptide bond formation was shown, ~2 s^{-1} for wildtype and all mutants (Burakovsky et al., 2010). Also here though, a possible effect would probably be masked by slow binding kinetics, since the experiments were performed at reagent concentrations far below saturation (Pape et al., 1998). Finally, *in vivo* mutagenesis of the corresponding bases in yeast ribosomes did not show any significant effect on growth rate (Rakauskaite and Dinman, 2011), further weakening the notion of aa-tRNAs slowly squeezing through the hypothetical "accommodation corridor".

The rate-accuracy trade-off in bacterial protein synthesis

The fundamental trade-off between the speed and accuracy by which the mRNA programmed ribosome selects aminoacyl-tRNAs in ternary complex with EF-Tu·GTP can be understood from elementary Michaelis–Menten kinetics. Translation accuracy depends not only on how well the ribosome discriminates a cognate from a non-cognate ternary complex in terms of different binding free energies ($\Delta\Delta G^0$) but also on how well the ribosome utilizes this difference to repress amino acid substitution errors. Most probably, the ribosome has evolved to maximize $\Delta\Delta G^0$, and thereby the intrinsic selectivity, by an optimal design of the binding pocket for the transition state of product formation, while the degree of utilization, determined by the discard parameters, has evolved to maximize the growth rate of bacteria (Ehrenberg and Kurland, 1984; Kurland and Ehrenberg, 1984). To illustrate this, we consider the following Michaelis-Menten scheme:

$$E + S^{c(nc)} \underset{k_d^{c(nc)}}{\overset{k_a^{c(nc)}}{\rightleftarrows}} ES^{c(nc)} \xrightarrow{k_c^{c(nc)}} E + P^{c(nc)} \tag{6}$$

The enzyme, E, binds a cognate, S^c, or non-cognate, S^{nc}, substrate with association rate constants k_a^c or k_a^{nc}, respectively. The enzyme-substrate complexes may dissociate with rate constants k_d^c or k_d^{nc}, respectively, or form products with rate constants k_c^c or k_c^{nc}, respectively. The steady-state flow of cognate product formation, j^c, is then (Fersht, 1999):

$$j^c = s^c \cdot e \cdot (k_{cat}/K_m)^c = s^c \cdot e \cdot k_a^c \frac{k_c^c}{k_c^c + k_d^c} = s^c \cdot e \cdot k_a^c \frac{1}{1+a}, \tag{7}$$

where s^c and e denote the concentration of cognate substrate and free enzyme, respectively. The discard parameter, or utilization parameter, a, is defined as the ratio k_d^c / k_c^c. Similarly, the steady-state flow of non-cognate product formation, j^{nc}, can be written as:

$$j^{nc} = s^{nc} \cdot e \cdot (k_{cat}/K_m)^{nc} = s^{nc} \cdot e \cdot k_a^{nc} \frac{k_c^{nc}}{k_c^{nc} + k_d^{nc}} = s^{nc} \cdot e \cdot k_a^{nc} \frac{1}{1+d_d \cdot a} \tag{8}$$

Here, the non-cognate discard parameter, k_d^{nc} / k_c^{nc}, is expressed as $d_d \cdot a$, *i.e.* it has the factor a in common with the cognate substrate and a factor d_d defining the difference between the cognate and non-cognate discard reactions. The normalized accuracy, A, defined as the cognate product flow divided by the non-cognate product flow at similar substrate concentrations, is then given by:

$$A = \frac{(k_{cat}/K_m)^c}{(k_{cat}/K_m)^{nc}} = d_a \frac{1+d_d \cdot a}{1+a} = \frac{d_a + d \cdot a}{1+a}, \tag{9}$$

where $d_a = k_a^c / k_a^{nc}$ and the total intrinsic discrimination, d, is given by $d = d_a \cdot d_d$. Hence, the total discrimination parameter, d, is defined by individual cognate and non-cognate rate constants as:

$$d = \frac{k_a^c}{k_a^{nc}} \cdot \frac{k_d^{nc}}{k_d^c} \cdot \frac{k_c^c}{k_c^{nc}} = e^{\Delta\Delta G^{\ddagger}/RT} \tag{10}$$

In the case of initial selection of tRNA on the ribosome, $\Delta\Delta G^{\ddagger}$ represents the difference in standard free energy of the transition state for GTP hydrolysis between non-cognate and cognate reactions (Fig. 4), including both the differences in binding free energy and the observed faster GTPase activation for cognate versus non-cognate substrate (Ogle and Ramakrishnan, 2005; Pape et al., 1999).

If the cognate discard parameter a is varied from small to large values while k_a^c, d_a and d remain constant, the accuracy, A, varies from its smallest value d_a to its largest value d (see Eq. 9), while the cognate efficiency, k_{cat}/K_m, varies from its largest value k_a^c at low a to zero when a goes to infinity (Eq. 7). Hence, by adjusting a, *e.g.* by mutations in the substrate binding pocket, the efficiency-accuracy trade-off can be tuned by evolution for optimal cell growth. In experiments for which these conditions are fulfilled there is a linear relation between $(k_{cat}/K_m)^c$ and the accuracy, A (Johansson et al., 2011):

$$(k_{cat}/K_m)^c = k_a^c \frac{d - A}{d - d_a} \tag{11}$$

Then, a plot of $(k_{cat}/K_m)^c$ as a function of A gives a straight line, which has a y value equal to k_a^c when A has its lowest value d_a, and intercepts the x-axis when A has its highest value, d. Furthermore, there is an equivalent linear relation between the inverse k_{cat}/K_m values for the non-cognate and cognate reactions:

$$\frac{1}{(k_{cat}/K_m)^{nc}} = \frac{d}{(k_{cat}/K_m)^c} - \frac{d - d_a}{k_a^c} \tag{12}$$

Here, a plot of $1/(k_{cat}/K_m)^{nc}$ versus $1/(k_{cat}/K_m)^c$ gives a straight line with slope d.

Trade-off theory applied to recent results (Paper III)

In paper III we analyzed recent advances in the ribosome field with respect to the rate-accuracy trade-off theory. From ratios of cognate to non-cognate rate constants for the discriminating steps, *i.e.* k_{-2} and k_3 (Fig. 13), in the detailed kinetic scheme of tRNA selection on the ribosome presented by M. Rodnina and colleagues (Gromadski and Rodnina, 2004), the maximal

discrimination parameter, *d*, can be calculated as 226,000. However, under the experimental conditions used (Gromadski and Rodnina, 2004), a mere factor of 60 out of this maximal discrimination is actually being utilized (Fig. 1A in paper III). This could suggest that indeed, the ribosome is very capable of discriminating similar substrates from each other, but this high discrimination is not needed and instead wasted to the benefit of rapid protein synthesis. On the other hand, as gets evident when considering an *in vivo* like situation where the cognate ternary complexes compete with an excess of non-cognate ternary complexes (concentrations taken from (Gromadski et al., 2006)), an increase of accuracy from 60 towards the maximal accuracy initially leads to *higher* protein synthesis rate, before the influence of the trade-off effect reduces the rate again (Fig. 1B, red line in paper III). This phenomenon is due to the inhibition of ribosomes by non-cognate substrates at low accuracy. Another seemingly suboptimal feature of the presented scheme (Gromadski and Rodnina, 2004) is the non-discriminating high affinity initial binding step. As can be seen by comparing the red line, calculated directly from the proposed scheme, with the blue line (Fig. 1B in paper III), where we have reduced the strong affinity by increasing the rate constants k_2 and k_{-1} by the same factor of 10,000, irrespective of substrate, this non-discriminating binding would strongly reduce the *in vivo* rate of protein synthesis. This kind of inhibitory effect, we proposed, could easily be prevented in nature by simply mutating the binding region of the ribosome and thereby decreasing the affinity of *all* ternary complexes to the same extent.

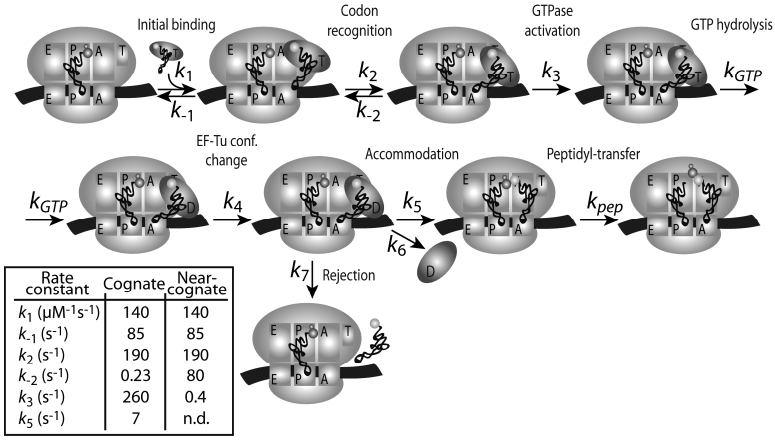

Rate constant	Cognate	Near-cognate
k_1 ($\mu M^{-1}s^{-1}$)	140	140
k_{-1} (s^{-1})	85	85
k_2 (s^{-1})	190	190
k_{-2} (s^{-1})	0.23	80
k_3 (s^{-1})	260	0.4
k_5 (s^{-1})	7	n.d.

Figure 13. Detailed scheme of tRNA selection on the ribosome (Gromadski and Rodnina, 2004).

Further, we also mention in the paper that one possible explanation for the seemingly high *d* value in (Gromadski and Rodnina, 2004) is that the cognate rate constant k_{-2} (Fig. 13) is underestimated. This argument is based

on the fact that the rate constant is determined from experiments where a yeast Phe-tRNA^{Phe}(Prf16/17)-containing ternary complex, either with the non-hydrolyzable GTP analogue GDPNP (Pape et al., 1999) or a GTPase deficient EF-Tu mutant (Gromadski and Rodnina, 2004), is pre-bound to initiated ribosomes, and then chased by non-fluorescent ternary complexes. The fluorescence signal decrease is supposed to represent the dissociation of the ternary complex from the codon recognition complex (Fig. 13), which according to the authors represents in the cognate case the rate constant k_{-2}, and in the non-cognate case a combination of k_{-2} and k_{-1}. However, in an earlier paper the authors declare that the GTPase deficient mutant proceeds all the way to GTPase activation (k_3): "This indicates that the mutation does not affect the GTPase-activation rearrangement, but rather inhibits subsequent steps." (Daviter et al., 2003), and results from single molecule FRET experiments in the laboratory of J. Puglisi suggest that the GDPNP containing ternary complex also enters a more stable state than the codon recognition complex (Blanchard et al., 2004). Hence, the experimental results from the chase experiments with the EF-Tu mutant or GDPNP, a technique that has also been used in subsequent studies from the same group (Gromadski et al., 2006; Kothe and Rodnina, 2007), and in the laboratory of R. Green (e.g. (Cochella and Green, 2005; Zaher and Green, 2010)), most probably do not properly represent tRNA selection on the ribosome with natural substrates. To this discussion it should also be added that a dissociation time from an internal state, such as the codon recognition complex and perhaps even more importantly the GTPase activated complex (Fig. 13), necessarily involves also the forward rate constants up to that state, which in this particular case are not negligible. For example, a ternary complex moving backwards with the rate constant k_{-2} in the scheme in figure 13 has a higher probability of going forward again and not fall off since k_2 in this case is bigger than k_{-1}. This is also one of the explanations why the proposed scheme suggests such strong inhibition of ribosomes by non-cognate aa-tRNAs.

Overall, the results from the analysis in paper III showed, somewhat counter intuitively, that *in vivo*, it is actually possible that an increase in accuracy of tRNA selection results in a more rapid protein synthesis due to less ribosome inhibition by non-cognate ternary complex. Together with the trade-off analysis this gives a hypothetical optimum where the deleterious effects of ribosome inhibition, and efficiency decrease due to high non-selective discard rate, are minimized. Finally, the results also suggested that there might be problems with the detailed kinetic scheme of ribosome function presented by the laboratory of M. Rodnina, and we also proposed an explanation to this in the form of a possible experimental artefact.

Experimental evidence for the rate-accuracy trade-off (Paper IV)

The simple trade-off analysis, implying a linear relation between efficiency and accuracy (Eq. 11) originates from experimental and theoretical work described nearly 30 years ago (Ehrenberg and Kurland, 1984; Kurland and Ehrenberg, 1984), but, due to lack of a suitable assay it was never tested experimentally. Since a variation in the discard parameter, *a*, with fixed *d* values and association rate constants, would be needed, it was not obvious how such experiments could be implemented. However, while trying to understand the differences between our results and those of others, *e.g.* from the experiments in paper I, we noticed that the only apparent divergence in the kinetics in the different systems was in the K_m, and the k_{cat}/K_m value. This together with observations of PEP concentration dependent variations in k_{cat}/K_m (Bouakaz, 2006; Johansson et al., 2011) made us try a series of k_{cat}/K_m determinations for GTP hydrolysis for a cognate ($tRNA^{Lys}$ on AAA) and a non-cognate ($tRNA^{Lys}$ on GAA, introducing a single U-G mismatch) reaction. Misreading by $tRNA^{Lys}$ was chosen because for this tRNA a thorough, systematic *in vivo* study of misreading had been conducted (Kramer and Farabaugh, 2007). To be able to see a hypothetically straight line, we realized that we needed to significantly improve the precision of the experiments performed with non-cognate tRNAs compared to how they had previously been performed (Bilgin et al., 1992). To some extent this was solved by the new method of separating nucleotides on an ion-exchange column rather than TLC, but the major improvement came from running a cognate reaction in parallel with the non-cognate reaction, *i.e.* the *very same* T_3 on GAA as well as AAA programmed ribosomes. Using this experimental approach, and by fitting the two experimental series together with four out of five parameters shared, we got precise and unambiguous estimates of the non-cognate k_{cat}/K_m values. The preliminary results showed, to our big surprise, a nearly perfect straight line when we plotted AAA reading efficiency versus the accuracy (AAA reading over GAA reading) according to equation 11 (Fig. 14, black squares). However, the method had one major obstacle, we could not go down in PEP concentration enough to reach the highest efficiency possible, for obvious reasons (less than zero is difficult…) and also because at low PEP concentrations the energy pump is dysfunctional, leading to poorly defined kinetics. In other words, another way of adjusting the *a* parameter was needed. The solution came from the realization that PEP is a weak Mg^{2+} chelator (Wold and Ballou, 1957). That is, the effect from the PEP titration was probably of secondary nature and what really mattered was the concentration of free Mg^{2+} ions, which had been known since long back to change the accuracy properties of the ribosome (Szer and Ochoa, 1964). Hence, the experiments with $tRNA^{Lys}$ reading AAA or GAA codons were repeated with different additions of Mg^{2+}

ions, 1 to 10 mM, to the standard polymix concentration of 5 mM, and the results were identical to those from the PEP titration (Fig. 14).

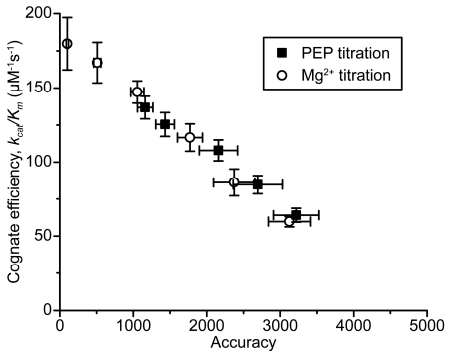

Figure 14. Trade-off plot for Lys-tRNA^{Lys} reading its completely matched AAA codon versus the single-mismatch GAA codon. k_{cat}/K_m values for GTP hydrolysis were measured for both cognate and non-cognate reactions at different concentrations of PEP or Mg^{2+} in the buffer.

So, it seemed we could, by titrating Mg^{2+} ions in the buffer, walk along the efficiency-accuracy trade-off line *in vitro*. What the Mg^{2+} ions are really doing is to me very difficult to tell. From the look of the cognate titration curve it seems as if some important Mg^{2+} binding site is being titrated, and that the k_{cat}/K_m saturates at approximately 180 $\mu M^{-1}s^{-1}$ (Fig. 3C in paper IV). However, the non-cognate reaction does not saturate at all in the same Mg^{2+} range, speaking against this hypothesis. A more plausible explanation is instead that the affinity of EF-Tu to the ribosome is modulated by changes in the Mg^{2+} concentration. However, for our analysis the molecular mechanism does not really matter. The important thing is whether the *d* parameter and the association rate constants remain fixed during the Mg^{2+} titration, when the *a* parameter is varied.

To explore the method further we tested the Mg^{2+} dependence of tRNA^{Lys} reading all possible single-mismatch codons. Since the method gives very precise measurements of relative efficiencies this was also interesting in the sense of efficiency variations of different mismatches. That is, would the accuracy level be the same on different codons, or without obvious pattern as suggested from earlier studies (Gromadski et al., 2006), or are there some general rules and patterns that govern the reading of the genetic code? Hence, k_{cat}/K_m values for tRNA^{Lys} reading all possible single-mismatch codons were determined at varying Mg^{2+} concentration. The results were plotted the same way as before, as the trade-off (Fig. 15A), but to simplify the parameter fitting (see Supporting Information in paper IV) we also made an equivalent plot where the inverted non-cognate k_{cat}/K_m values were plotted versus the inverted cognate k_{cat}/K_m values (Fig. 15B). All data were fitted together according to equation 12. Since the intercept with the x-axis

in figure 15B is, without parameter fitting, the same for all series and equal to the inverse of the cognate plateau (Fig. 3C in paper IV), there seems to be no substantial selection in the binding reaction, *i.e.* $d_a << d$ (see Eq. 12). Previous experiments at 20°C and higher concentration of free Mg^{2+} than used here also suggest that $d_a \approx 1$ (Gromadski and Rodnina, 2004), why we used $d_a = 1$ in equation 12 during our parameter estimation. From the results a number of interesting observations were made. First of all, for all nine series the data fit very well with the straight line model (Figs. 15A and 15B) indicating that the *d* values and association rate constants indeed remained constant during the Mg^{2+} titration. This is important for the interpretation of the results with respect to *in vivo* accuracies, and implies that we did estimate the maximal accuracies that governs the trade-off tuning in living cells. Further, despite the rather modest variations in the *d* values, ranging from 1,500 (for misreading of AAU) to about 25,000 (for misreading of ACA), we did see clear patterns arguing against the previously suggested "uniform response to mismatches" (Gromadski et al., 2006). The *d* value corresponding to a particular mismatch was highest in the second, intermediate in the first and smallest in the third codon position, which fits well with the proposed geometrical sensing of the first two codon positions but not of the third (Fourmy et al., 1996; Fourmy et al., 1998; Ogle et al., 2001; Ogle and Ramakrishnan, 2005), and with the observation that the second codon position plays the largest role in determining the chemical properties of incorporated amino acids (Alff-Steinberger, 1969). The *d* value corresponding to misreading at a particular codon position was in general highest for the U:C, intermediate for the U:U and smallest for the U:G mismatch (Fig. 15C). Finally, the third position U:G mismatch, considered as cognate to $tRNA^{Lys}$, was ten times less efficient than reading of the completely matched codon AAA.

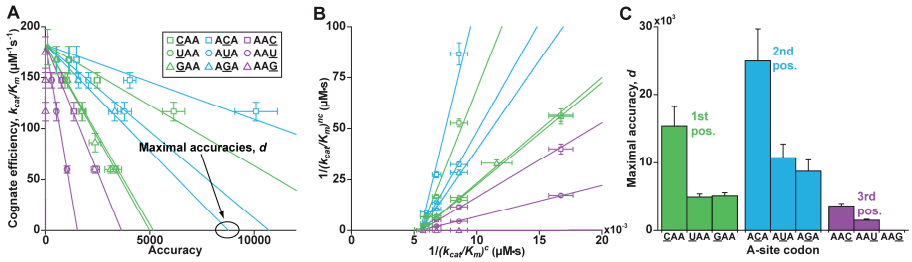

Figure 15. The rate-accuracy trade-off in initial selection. (*A*) Rate-accuracy trade-off lines as plots of the cognate k_{cat}/K_m (AAA codon) versus the accuracy (calculated as the ratio of the cognate k_{cat}/K_m to the non-cognate k_{cat}/K_m) on all single-mismatch codons read by $tRNA^{Lys}$. The maximal accuracy, *d*, is in each case determined by the intercept of the line with the x-axis. (*B*) The inverted non-cognate k_{cat}/K_m plotted versus the inverted cognate k_{cat}/K_m at different Mg^{2+} concentrations. The slopes of the straight lines give the maximal accuracy, *d*, for all nine single-mismatch codons (see Eq. 12). Symbols as in panel A. (*C*) *d* values as estimated from linear fits shown in panel B.

Additionally, we performed experiments to estimate the overall accuracy, including proofreading, for one mismatch reading case. Here, k_{cat}/K_m for fMet-Lys dipeptide formation when $tRNA^{Lys}$ misreads a GAA codon was estimated at different Mg^{2+} concentrations. The overall accuracy was then calculated as the ratio between cognate and non-cognate dipeptide formation efficiencies at different Mg^{2+} concentrations, where the cognate dipeptide efficiency was assumed to be the same as the cognate GTP hydrolysis efficiency. The latter assumption is correct if the cognate substrate is not proofread to any significant level, and if one GTP is hydrolysed per tRNA passing through initial selection, which seems to be the case (Rodnina and Wintermeyer, 1995). The resulting trade-off plot is shown in figure 16. The overall accuracy varies between 700 and 150,000 in our Mg^{2+} titration. By comparing this trade-off curve to measured misreading of the same codon-anticodon pair *in vivo* (Kramer and Farabaugh, 2007), normalized to the tRNA abundancy in the cell, we could then tell where on the trade-off curve we represent the *in vivo* accuracy best, *i.e.* at around 98 % maximal efficiency. The specific mismatch reading, however, is most probably over estimated *in vivo* due to background luminescence (Kramer and Farabaugh, 2007), why we rather regard this value as an upper limit to the actual error *in vivo*. Another calibration method would be to compare actual levels of Mg^{2+} *in vivo* and *in vitro*. The concentration of free Mg^{2+} ions in the *E. coli* cell has been estimated to be in the 1 to 2 mM range (Alatossava et al., 1985). In our experiments, the free Mg^{2+} concentration is estimated to range between 1.3 and 7.5 mM (see Discussion in paper IV). This comparison suggests the *in vivo* accuracy to be much higher, at the cost of efficiency with cognate k_{cat}/K_m values less than 60% of their maximal values.

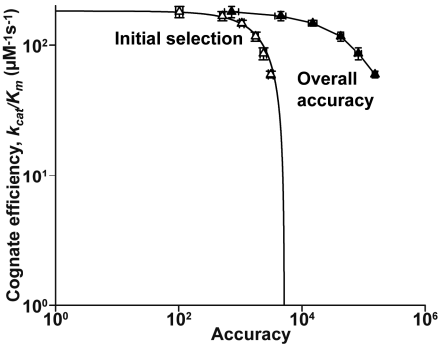

Figure 16. Rate-accuracy trade-off plots in log-log scale for initial selection (Δ) and overall accuracy (▲) for Lys-tRNA^{Lys} selection of the AAA in relation to the GAA codon. The initial selection is the same as plotted in linear scale in figure 15A.

In conclusion, the experimental results in paper IV fit very well with the simple trade-off model perceived almost three decades ago (Ehrenberg and Kurland, 1984; Kurland and Ehrenberg, 1984). Thus, it seems that there is a linear trade-off between efficiency and accuracy of genetic code reading by the ribosome, and by varying the Mg^{2+} concentration in our *in vitro* translation system we can travel along such trade-off lines. Exploiting this feature, we estimated maximal accuracies, *d* values, for a complete set of single mismatches for one tRNA species. The *d* values are themselves important for understanding the trade-off *in vivo*, and can also be used for calibration of *in vitro* translation systems to translation in the living cell. Additionally, the patterns of codon reading, apparent in figure 15C, with second codon position most tightly and third codon position least tightly controlled, fit well with the observation that the second codon position is most important in determining the chemical properties of the encoded amino acid (Alff-Steinberger, 1969), but also with the geometrical sensing hypothesis stipulating highest reading accuracy in the two first codon positions (Ogle and Ramakrishnan, 2005).

Conclusions and future outlook

The first two papers in this thesis deal with the rate of ribosomal peptide bond formation. We were concerned about the apparent lack of consistency between recent *in vitro* experimental results on protein synthesis and the rate of protein synthesis in the living *E. coli* cell. Therefore we set off to measure the rate of peptide bond formation, along with the accuracy, in our optimized *in vitro* protein synthesis system, and we could show that indeed *in vitro* protein synthesis can be as rapid and as accurate as in the living cell. However, when trying to reproduce the slow kinetics of the seemingly suboptimal buffer system used by others we also got *in vivo* comparable results, indicating a possible artefact, either in our experiments or in theirs. In addition, we also challenged the commonly held view that tRNA accommodation is limiting the rate of peptide bond formation on the ribosome. To our minds there was no obvious reason why the approximately 90 Å movement of a molecule (Whitford et al., 2010) would take 100 ms, especially considering the enormous selection pressure *in vivo* on the rate of protein synthesis. Also, we were not particularly convinced by the original experiments leading up to the notion of accommodation limited peptidyl transfer. In line with our suspicion, the measured temperature and pH dependence of the compounded accommodation and peptidyl transfer rate were pointing toward chemistry limiting peptidyl transfer. It could, of course, be that tRNA accommodation has exactly the same activation enthalpy and entropy as has been suggested for the chemical step of peptidyl transfer, and there could be a pH dependence in tRNA accommodation, that varies with the aa-tRNA and also with only one group being titrated as for the proposed mechanism of peptidyl transfer. Yet, since no quantitative data for accommodation exist, the most straight-forward interpretation must be that the chemistry of peptidyl transfer is not masked by slow tRNA accommodation. Hence, from the results in papers I and II we are optimistic that we have opened up the possibility to study, with natural substrates, one of the most fundamental chemical reactions of life itself, the ribosome catalyzed peptidyl transfer.

In papers III and IV we investigated the proposed rate-accuracy trade-off in protein synthesis. We first evaluated recent biochemical advances with respect to our simple trade-off model and found that protein synthesis seemed remarkably suboptimal with respect to rate *and* accuracy. To us it appeared as a simple tuning of the system would increase both rate and

accuracy, why we argued that the biochemical results did not reflect *in vivo* protein synthesis very well since in the living cell the parameters that govern the rate and the accuracy of protein synthesis are under high selection pressure and therefore most probably are optimized accordingly.

Furthermore, we developed a method to tune the rate-accuracy trade-off in our *in vitro* protein synthesis system by varying the concentration of Mg^{2+} ions in the buffer. We found a linear relation between efficiency (rate) and accuracy of initial tRNA selection in accordance with our proposed model. Utilizing this method for a complete set of single-mismatch interactions we could estimate maximal accuracy limits, and found clear patterns of misreading frequencies depending on mismatch position and identity. For one mismatch case we also measured how the overall accuracy, including proofreading, varies with efficiency, and by comparing this result to known error frequencies *in vivo*, we could make a first attempt to calibrate *in vitro* experiments to protein synthesis in the living cell.

The experimental method developed is very sensitive compared to earlier setups, and we are optimistic that it can be used to shed light also on many other aspects of accuracy of codon reading in the cell. For example, by expanding the study to include a few more tRNAs, it may be possible to estimate mismatch reading frequencies of all tRNAs on all codons, and hence, together with known *in vivo* tRNA concentrations, make a complete model for genetic code reading and misreading in the living cell. This, together with investigation of codon reading by non- or under-modified tRNAs will also give insight into the evolution of the genetic code, and how the accuracy in living cells has been evolutionarily tuned for maximal fitness of growing bacteria. Finally, the method can hopefully also be used to clarify the mechanism of action of, and resistance mechanisms against, several clinically important antibiotic drugs affecting the accuracy of genetic code reading.

Summary in Swedish

Alla levande celler är uppbyggda, organiserade och kontrollerade av proteiner. Proteiner bygger upp t ex hår och muskler, fungerar som receptorer i cellväggarna för att överföra externa signaler till cellens insida, transporterar molekyler från en del av kroppen eller cellen till en annan och, kanske viktigast av allt, katalyserar och kontrollerar i stort sett alla kemiska reaktioner som sker inuti en levande cell. Proteiner består av långa aminosyrekedjor (polypeptider) vars sekvenser bestäms av gener lagrade i cellerna som DNA, vilka kopieras till budbärar-RNA (mRNA) som i sin tur läses av cellernas proteinsyntesmaskineri, ribosomerna (Fig. 1). Ribosomerna binder till mRNA-molekylerna, där nukleotidsekvensen som utgör mRNA:t avkodas genom att tripletter av nukleotider binder till komplementära nukleotid-tripletter på transport-RNA molekyler (tRNA). Varje tRNA-typ för med sig en specifik aminosyra enligt den genetiska koden (Fig. 2), och på så vis läser ribosomen mRNA:t, tre nukleotider åt gången, och sätter ihop aminosyrorna enligt den ursprungliga mallen på DNA:t. Allt liv på jorden förutsätter inte bara snabb, utan också noggrann kodöversättning, så att aminosyror inte sätts in på fel platser i cellernas proteiner.

De första två artiklarna i avhandlingen (Paper I och II) behandlar hastigheten hos bakteriell proteinsyntes. Vi var bekymrade över bristen på överensstämmelse mellan senare års resultat från *in vitro*-experiment och proteinsyntesen i levande celler. Vi beslutade oss därför för att mäta hastighet och noggrannhet hos proteinsyntesen i vårt optimerade *in vitro*-system och fann att det visst gick att få proteinsyntes *in vitro* som var lika snabb och noggrann som *in vivo*. Vidare ifrågasatte vi den gängse uppfattningen att tRNA-ackommodering (när tRNA:t svänger in med den aminosyrabundna änden mot det katalytiska sätet i ribosomen efter korrekt kod-igenkänning) skulle vara det hastighetsbegränsande steget vid proteinsyntes på ribosomen, och inte själva det kemiska steget varvid en ny peptidbindning bildas mellan den inkommande aminosyran och den tidigare syntetiserade polypeptiden. Vi såg ingen självklar anledning till varför en ca 90 Å förflyttning av en molekyl skulle behöva ta 100 ms, framförallt med tanke på det oerhörda evolutionära selektionstryck som finns på proteinsyntesen. Vi var heller inte speciellt övertygade av de ursprungliga experimenten där den långsamma tRNA-ackommoderingen upptäcktes. I överensstämmelse med vår misstanke pekade också vårt uppmätta

temperaturberoende (Fig. 10 och Table 1) och vårt uppmätta pH-beroende (Fig. 11 och Table 2) av peptidbindningsreaktionen mot hastighets-begränsning från själva kemin. Självklart skulle det kunna vara så att tRNA-ackommodering också har exakt samma aktiveringsentalpi och -entropi som föreslagits för det kemiska steget i peptidbindningsformering, och det skulle också kunna vara så att tRNA-ackommodering har ett pH-beroende som varierar med inkommande aminoacyl-tRNA och där endast en reaktionsessentiell grupp titreras med pH, men eftersom inga kvantitativa data existerar för tRNA-ackommodering måste den mest rimliga tolkningen ändå vara att ribosomal peptidbindningsformering *inte* begränsas av någon långsam ackommodering av tRNA. Alltså, utifrån de två studierna tror vi att vi öppnat upp möjligheten att studera, med naturliga substrat, en av de mest fundamentala kemiska reaktionerna i livet självt, ribosomal peptidbindnings-formering.

I de följande två artiklarna (Paper III och IV) undersökte vi den kompromiss mellan hastighet och noggrannhet i proteinsyntesen som nödvändigtvis finns i levande celler. Först analyserade vi de senaste biokemiska framstegen i fältet med utgångspunkt i vår enkla matematiska modell för hastighets-noggrannhets-kompromissen. Vi fann att dessa experiment tycktes tyda på en proteinsyntes som är anmärkningsvärt suboptimal vad beträffar *både* hastighet och noggrannhet. För oss verkade det som att en enkel justering av systemet skulle öka både hastigheten och noggrannheten, varför vi argumenterade för att de biokemiska experimenten inte representerade *in vivo* proteinsyntes speciellt väl eftersom de parametrar som styr hastighet och noggrannhet i en levande cell är under högt selektionstryck och därför mest troligast justerade för en optimal lösning av hastighets-noggrannhets-problemet.

Vidare utvecklade vi en metod, som bygger på variation av koncentrationen av Mg^{2+}-joner i bufferten, för att justera kompromissen mellan hastighet och noggrannhet i vårt *in vitro*-system för proteinsyntes. Vi fann ett linjärt samband mellan effektivitet (hastighet) och noggrannhet i initialselektionen av tRNA (Fig. 14) i enlighet med vår matematiska modell. Genom att använda denna metod kunde vi, för en komplett uppsättning av en-bas-felläsningar, estimera maximala noggrannhetsgränser (Fig. 15A), och vi fann också tydliga mönster för felläsning beroende på typ och position av felet i kodordet (Fig. 15C). För en specifik felläsning mätte vi också hur den totala noggrannheten (inkluderande korrekturläsningsmekanismen som följer på initialselektionen) varierar med effektiviteten (Fig. 16), och kunde genom jämförelser med kända felläsningsfrekvenser *in vivo* göra ett första försök att kalibrera *in vitro*-experiment med proteinsyntesen i en levande cell mer exakt.

Den utvecklade metoden är mycket känslig i jämförelse med tidigare mätningar, och vi hoppas att med denna metod i framtiden kunna belysa flera aspekter vad gäller noggrannhet i cellernas kodläsning. Till exempel,

genom att utöka studien med ytterligare några tRNA-typer bör vi kunna uppskatta felläsningsfrekvenser för alla tRNA-typer på alla möjliga kodord, och på så vis kunna göra en fullständig modell för hur den genetiska koden läses och felläses i en levande cell. Tillsammans med undersökningar av hur de talrika kemiska modifieringar som finns på tRNA-molekyler påverkar kodläsningen, kommer vi förhoppningsvis också att kunna säga något om hur den genetiska koden uppkommit och finjusterats genom evolution, och hur noggrannheten i kodläsningen optimerats för maximal tillväxt för levande bakterier. Slutligen kommer metoden förhoppningsvis också att kunna ge nya insikter om verkningsmekanismer för, och resistens-mekanismer mot, flera kliniskt relevanta antibiotiska preparat som påverkar noggrannheten i läsningen av den genetiska koden.

Acknowledgements

My deepest gratitude goes to my supervisor **Måns**. Thank you for sharing your passion for science, and for all the interesting discussions we had over the years, ranging from otters and super-heroes to Sarakatsani and Eeyore. You are a brilliant scientist and it has been a great pleasure to learn from you.

I would also like to express my warmest thanks to:

The Ehrenberg group – in particular **Martin**, I owe you a great deal for introducing me to the noble art of pipetting and experimental design. It was invaluable and gave me a flying start; **Misha**, for knowing so much and, sometimes, sharing this wisdom; **David** for all the discussions over the years; **Vasili**, see you at the next conference; **Elli** for bringing me into the accuracy business, **Anneli** for feedback on anything related to science or life and for meticulous proofreading of the thesis; **Kaweng** for finishing the pH paper when I was at home changing diapers; **Jingji** for the work on our joint published work and ongoing projects.

The Molecular Biology Program – **Suparna** and **Tony** for scientific input.

Past and present colleagues at the **Department of Cell and Molecular Biology** – in particular **Johan Åqvist** for collaborations, discussions and your willingness and eagerness to explain all the chemistry; **Erik**, we have shared a lot. Thanks for scientific/non-scientific discussions over the years.

My **friends, family and extended family** – Who with their different backgrounds and interests have enriched my life and helped me put my scientific work into perspective.

My **parents** – For their never ending encouragement and support.

My **brother** – For leading the way.

Finally, I would like to thank my wife **Anna** and our wonderful children **Bertil** and **Märta** who fill my life with so much love and joy. You are the best!

References

Alatossava, T., Jutte, H., Kuhn, A., and Kellenberger, E. (1985). Manipulation of intracellular magnesium content in polymyxin B nonapeptide-sensitized Escherichia coli by ionophore A23187. J Bacteriol *162*, 413-419.

Alff-Steinberger, C. (1969). The genetic code and error transmission. Proc Natl Acad Sci U S A *64*, 584-591.

Ban, N., Nissen, P., Hansen, J., Moore, P.B., and Steitz, T.A. (2000). The complete atomic structure of the large ribosomal subunit at 2.4 A resolution. Science *289*, 905-920.

Beringer, M., Bruell, C., Xiong, L., Pfister, P., Bieling, P., Katunin, V.I., Mankin, A.S., Bottger, E.C., and Rodnina, M.V. (2005). Essential mechanisms in the catalysis of peptide bond formation on the ribosome. J Biol Chem *280*, 36065-36072.

Beringer, M., and Rodnina, M.V. (2007). Importance of tRNA interactions with 23S rRNA for peptide bond formation on the ribosome: studies with substrate analogs. Biol Chem *388*, 687-691.

Bieling, P., Beringer, M., Adio, S., and Rodnina, M.V. (2006). Peptide bond formation does not involve acid-base catalysis by ribosomal residues. Nat Struct Mol Biol *13*, 423-428.

Bilgin, N., Claesens, F., Pahverk, H., and Ehrenberg, M. (1992). Kinetic properties of Escherichia coli ribosomes with altered forms of S12. J Mol Biol *224*, 1011-1027.

Bjare, U., and Gorini, L. (1971). Drug dependence reversed by a ribosomal ambiguity mutation, ram, in Escherichia coli. J Mol Biol *57*, 423-435.

Bjorkman, J., Samuelsson, P., Andersson, D.I., and Hughes, D. (1999). Novel ribosomal mutations affecting translational accuracy, antibiotic resistance and virulence of Salmonella typhimurium. Mol Microbiol *31*, 53-58.

Blanchard, S.C., Gonzalez, R.L., Kim, H.D., Chu, S., and Puglisi, J.D. (2004). tRNA selection and kinetic proofreading in translation. Nat Struct Mol Biol *11*, 1008-1014.

Bouadloun, F., Donner, D., and Kurland, C.G. (1983). Codon-specific missense errors in vivo. Embo J *2*, 1351-1356.

Bouakaz, E. (2006). Choice of tRNA on translating ribosomes (Uppsala: Acta Universitatis Upsaliensis : Universitetsbiblioteket).

Bremer, H., and Dennis, P.P. (2008). Modulation of Chemical Composition and Other Parameters of the Cell at Different Exponential Growth Rates. In EcoSal-Escherichia coli and Salmonella: Cellular and Molecular Biology. http://www.ecosal.org, A. Böck, R. Curtiss III, J.B. Kaper, P.D. Karp, F.C. Neidhardt, T. Nyström, J.M. Slauch, C.L. Squires, D. Ussery, and E. Schaechter, eds. (Washington, DC: ASM press).

Brownstein, B.L., and Lewandowski, L.J. (1967). A mutation suppressing streptomycin dependence. I. An effect on ribosome function. J Mol Biol *25*, 99-109.

Brunelle, J.L., Youngman, E.M., Sharma, D., and Green, R. (2006). The interaction between C75 of tRNA and the A loop of the ribosome stimulates peptidyl transferase activity. Rna *12*, 33-39.

Burakovsky, D.E., Sergiev, P.V., Steblyanko, M.A., Kubarenko, A.V., Konevega, A.L., Bogdanov, A.A., Rodnina, M.V., and Dontsova, O.A. (2010). Mutations at the accommodation gate of the ribosome impair RF2-dependent translation termination. Rna *16*, 1848-1853.

Chakrabarti, S., and Gorini, L. (1975). Growth of bacteriophages MS2 and T7 on streptomycin-resistant mutants of Escherichia coli. J Bacteriol *121*, 670-674.

Cochella, L., and Green, R. (2005). An active role for tRNA in decoding beyond codon:anticodon pairing. Science *308*, 1178-1180.

Crick, F.H. (1966). Codon--anticodon pairing: the wobble hypothesis. J Mol Biol *19*, 548-555.

Daviter, T., Wieden, H.J., and Rodnina, M.V. (2003). Essential role of histidine 84 in elongation factor Tu for the chemical step of GTP hydrolysis on the ribosome. J Mol Biol *332*, 689-699.

Ehrenberg, M., and Kurland, C.G. (1984). Costs of accuracy determined by a maximal growth rate constraint. Q Rev Biophys *17*, 45-82.

Ermolenko, D.N., and Noller, H.F. (2011). mRNA translocation occurs during the second step of ribosomal intersubunit rotation. Nat Struct Mol Biol *18*, 457-462.

Fersht, A. (1999). Structure and mechanism in protein science : a guide to enzyme catalysis and protein folding (New York: Freeman and Company).

Fersht, A.R., and Dingwall, C. (1979). Evidence for the double-sieve editing mechanism in protein synthesis. Steric exclusion of isoleucine by valyl-tRNA synthetases. Biochemistry *18*, 2627-2631.

Fourmy, D., Recht, M.I., Blanchard, S.C., and Puglisi, J.D. (1996). Structure of the A site of Escherichia coli 16S ribosomal RNA complexed with an aminoglycoside antibiotic. Science *274*, 1367-1371.

Fourmy, D., Yoshizawa, S., and Puglisi, J.D. (1998). Paromomycin binding induces a local conformational change in the A-site of 16 S rRNA. J Mol Biol *277*, 333-345.

Frank, J., and Agrawal, R.K. (2000). A ratchet-like inter-subunit reorganization of the ribosome during translocation. Nature *406*, 318-322.

Gorini, L., Jacoby, G.A., and Breckenridge, L. (1966). Ribosomal ambiguity. Cold Spring Harb Symp Quant Biol *31*, 657-664.

Gromadski, K.B., Daviter, T., and Rodnina, M.V. (2006). A uniform response to mismatches in codon-anticodon complexes ensures ribosomal fidelity. Mol Cell *21*, 369-377.

Gromadski, K.B., and Rodnina, M.V. (2004). Kinetic determinants of high-fidelity tRNA discrimination on the ribosome. Mol Cell *13*, 191-200.

Hansen, J.L., Schmeing, T.M., Moore, P.B., and Steitz, T.A. (2002). Structural insights into peptide bond formation. Proc Natl Acad Sci U S A *99*, 11670-11675.

Hesslein, A.E., Katunin, V.I., Beringer, M., Kosek, A.B., Rodnina, M.V., and Strobel, S.A. (2004). Exploration of the conserved A+C wobble pair within the ribosomal peptidyl transferase center using affinity purified mutant ribosomes. Nucleic Acids Res *32*, 3760-3770.

Hopfield, J.J. (1974). Kinetic proofreading: a new mechanism for reducing errors in biosynthetic processes requiring high specificity. Proc Natl Acad Sci U S A *71*, 4135-4139.

Jelenc, P.C., and Kurland, C.G. (1979). Nucleoside triphosphate regeneration decreases the frequency of translation errors. Proc Natl Acad Sci U S A *76*, 3174-3178.

Johansson, M., Ieong, K.W., Åqvist, J., Pavlov, M.Y., and Ehrenberg, M. (2011). Rate and accuracy of messenger RNA translation on the ribosome. In

Ribosomes: Structure, Function, and Dynamics, M. Rodnina, W. Wintermeyer, and R. Green, eds. (WienNew York: Springer-Verlag).

Katunin, V.I., Muth, G.W., Strobel, S.A., Wintermeyer, W., and Rodnina, M.V. (2002). Important contribution to catalysis of peptide bond formation by a single ionizing group within the ribosome. Mol Cell *10*, 339-346.

Kothe, U., and Rodnina, M.V. (2007). Codon reading by tRNAAla with modified uridine in the wobble position. Mol Cell *25*, 167-174.

Kramer, E.B., and Farabaugh, P.J. (2007). The frequency of translational misreading errors in E. coli is largely determined by tRNA competition. Rna *13*, 87-96.

Kurland, C.G., and Ehrenberg, M. (1984). Optimization of translation accuracy. Prog Nucleic Acid Res Mol Biol *31*, 191-219.

Kurland, C.G., and Ehrenberg, M. (1985). Constraints on the accuracy of messenger RNA movement. Q Rev Biophys *18*, 423-450.

Liang, S.T., Xu, Y.C., Dennis, P., and Bremer, H. (2000). mRNA composition and control of bacterial gene expression. J Bacteriol *182*, 3037-3044.

Neidhardt, F.C. (1987). Escherichia coli and Salmonella typhimurium : cellular and molecular biology (Washington, D.C.: American Society for Microbiology).

Ninio, J. (1975). Kinetic amplification of enzyme discrimination. Biochimie *57*, 587-595.

Nissen, P., Hansen, J., Ban, N., Moore, P.B., and Steitz, T.A. (2000). The structural basis of ribosome activity in peptide bond synthesis. Science *289*, 920-930.

Ogle, J.M., Brodersen, D.E., Clemons, W.M., Jr., Tarry, M.J., Carter, A.P., and Ramakrishnan, V. (2001). Recognition of cognate transfer RNA by the 30S ribosomal subunit. Science *292*, 897-902.

Ogle, J.M., and Ramakrishnan, V. (2005). Structural insights into translational fidelity. Annu Rev Biochem *74*, 129-177.

Ozaki, M., Mizushima, S., and Nomura, M. (1969). Identification and functional characterization of the protein controlled by the streptomycin-resistant locus in E. coli. Nature *222*, 333-339.

Pan, D., Kirillov, S.V., and Cooperman, B.S. (2007). Kinetically competent intermediates in the translocation step of protein synthesis. Mol Cell *25*, 519-529.

Pape, T., Wintermeyer, W., and Rodnina, M. (1999). Induced fit in initial selection and proofreading of aminoacyl-tRNA on the ribosome. Embo J *18*, 3800-3807.

Pape, T., Wintermeyer, W., and Rodnina, M.V. (1998). Complete kinetic mechanism of elongation factor Tu-dependent binding of aminoacyl-tRNA to the A site of the E. coli ribosome. Embo J *17*, 7490-7497.

Parker, J. (1989). Errors and alternatives in reading the universal genetic code. Microbiol Rev *53*, 273-298.

Parmeggiani, A., and Swart, G.W. (1985). Mechanism of action of kirromycin-like antibiotics. Annu Rev Microbiol *39*, 557-577.

Pauling, L. (1957). The Probability of Errors in the Process of Synthesis of Protein Molecules. In Festschrift Arthur Stoll (Basel: Birkhäuse Verlag), pp. 597-602.

Pavlov, M.Y., and Ehrenberg, M. (1996). Rate of translation of natural mRNAs in an optimized in vitro system. Arch Biochem Biophys *328*, 9-16.

Pavlov, M.Y., Watts, R.E., Tan, Z., Cornish, V.W., Ehrenberg, M., and Forster, A.C. (2009). Slow peptide bond formation by proline and other N-alkylamino acids in translation. Proc Natl Acad Sci U S A *106*, 50-54.

Rakauskaite, R., and Dinman, J.D. (2011). Mutations of highly conserved bases in the peptidyltransferase center induce compensatory rearrangements in yeast ribosomes. Rna *17*, 855-864.

Rodnina, M.V., Fricke, R., and Wintermeyer, W. (1994). Transient conformational states of aminoacyl-tRNA during ribosome binding catalyzed by elongation factor Tu. Biochemistry *33*, 12267-12275.

Rodnina, M.V., Savelsbergh, A., Katunin, V.I., and Wintermeyer, W. (1997). Hydrolysis of GTP by elongation factor G drives tRNA movement on the ribosome. Nature *385*, 37-41.

Rodnina, M.V., and Wintermeyer, W. (1995). GTP consumption of elongation factor Tu during translation of heteropolymeric mRNAs. Proc Natl Acad Sci U S A *92*, 1945-1949.

Russell, J.B., and Cook, G.M. (1995). Energetics of bacterial growth: balance of anabolic and catabolic reactions. Microbiol Rev *59*, 48-62.

Ruusala, T., Ehrenberg, M., and Kurland, C.G. (1982). Is there proofreading during polypeptide synthesis? EMBO J *1*, 741-745.

Sanbonmatsu, K.Y., Joseph, S., and Tung, C.S. (2005). Simulating movement of tRNA into the ribosome during decoding. Proc Natl Acad Sci U S A *102*, 15854-15859.

Schluenzen, F., Tocilj, A., Zarivach, R., Harms, J., Gluehmann, M., Janell, D., Bashan, A., Bartels, H., Agmon, I., Franceschi, F., and Yonath, A. (2000). Structure of functionally activated small ribosomal subunit at 3.3 angstroms resolution. Cell *102*, 615-623.

Schmeing, T.M., Huang, K.S., Kitchen, D.E., Strobel, S.A., and Steitz, T.A. (2005). Structural insights into the roles of water and the 2' hydroxyl of the P site tRNA in the peptidyl transferase reaction. Mol Cell *20*, 437-448.

Schmeing, T.M., and Ramakrishnan, V. (2009). What recent ribosome structures have revealed about the mechanism of translation. Nature *461*, 1234-1242.

Schroeder, G.K., and Wolfenden, R. (2007). The rate enhancement produced by the ribosome: an improved model. Biochemistry *46*, 4037-4044.

Sievers, A., Beringer, M., Rodnina, M.V., and Wolfenden, R. (2004). The ribosome as an entropy trap. Proc Natl Acad Sci U S A *101*, 7897-7901.

Szer, W., and Ochoa, S. (1964). Complexing Ability and Coding Properties of Synthetic Polynucleotides. J Mol Biol *8*, 823-834.

Thompson, R.C., and Stone, P.J. (1977). Proofreading of the codon-anticodon interaction on ribosomes. Proc Natl Acad Sci U S A *74*, 198-202.

Trobro, S., and Åqvist, J. (2005). Mechanism of peptide bond synthesis on the ribosome. Proc Natl Acad Sci U S A *102*, 12395-12400.

Trobro, S., and Åqvist, J. (2006). Analysis of predictions for the catalytic mechanism of ribosomal peptidyl transfer. Biochemistry *45*, 7049-7056.

Tubulekas, I., and Hughes, D. (1993). Suppression of rpsL phenotypes by tuf mutations reveals a unique relationship between translation elongation and growth rate. Mol Microbiol *7*, 275-284.

Wagner, E.G., Jelenc, P.C., Ehrenberg, M., and Kurland, C.G. (1982). Rate of elongation of polyphenylalanine in vitro. Eur J Biochem *122*, 193-197.

Whitford, P.C., Onuchic, J.N., and Sanbonmatsu, K.Y. (2010). Connecting energy landscapes with experimental rates for aminoacyl-tRNA accommodation in the ribosome. J Am Chem Soc *132*, 13170-13171.

Wimberly, B.T., Brodersen, D.E., Clemons, W.M., Jr., Morgan-Warren, R.J., Carter, A.P., Vonrhein, C., Hartsch, T., and Ramakrishnan, V. (2000). Structure of the 30S ribosomal subunit. Nature *407*, 327-339.

Wohlgemuth, I., Pohl, C., and Rodnina, M.V. (2010). Optimization of speed and accuracy of decoding in translation. Embo J *29*, 3701-3709.

Wold, F., and Ballou, C.E. (1957). Studies on the enzyme enolase. I. Equilibrium studies. J Biol Chem *227*, 301-312.

Yamane, T., and Hopfield, J.J. (1977). Experimental evidence for kinetic proofreading in the aminoacylation of tRNA by synthetase. Proc Natl Acad Sci U S A *74*, 2246-2250.

Youngman, E.M., Brunelle, J.L., Kochaniak, A.B., and Green, R. (2004). The active site of the ribosome is composed of two layers of conserved nucleotides with distinct roles in peptide bond formation and peptide release. Cell *117*, 589-599.

Zaher, H.S., and Green, R. (2009). Quality control by the ribosome following peptide bond formation. Nature *457*, 161-166.

Zaher, H.S., and Green, R. (2010). Hyperaccurate and error-prone ribosomes exploit distinct mechanisms during tRNA selection. Mol Cell *39*, 110-120.

Zaher, H.S., and Green, R. (2011). A primary role for release factor 3 in quality control during translation elongation in Escherichia coli. Cell *147*, 396-408.

Zimmermann, R.A., Garvin, R.T., and Gorini, L. (1971). Alteration of a 30S ribosomal protein accompanying the ram mutation in Escherichia coli. Proc Natl Acad Sci U S A *68*, 2263-2267.

Acta Universitatis Upsaliensis

Digital Comprehensive Summaries of Uppsala Dissertations from the Faculty of Science and Technology 910

Editor: The Dean of the Faculty of Science and Technology

A doctoral dissertation from the Faculty of Science and Technology, Uppsala University, is usually a summary of a number of papers. A few copies of the complete dissertation are kept at major Swedish research libraries, while the summary alone is distributed internationally through the series Digital Comprehensive Summaries of Uppsala Dissertations from the Faculty of Science and Technology.

Distribution: publications.uu.se
urn:nbn:se:uu:diva-171040

ACTA
UNIVERSITATIS
UPSALIENSIS
UPPSALA
2012